

# Space-time finite element approximation of the Biot poroelasticity system with iterative coupling

M. Bause\*, F. A. Radu<sup>†</sup>, U. Köcher<sup>‡</sup>

\* <sup>‡</sup> Helmut Schmidt University, Faculty of Mechanical Engineering, Holstenhofweg 85,  
220433 Hamburg, Germany

<sup>†</sup> University of Bergen, Department of Mathematics, Allégaten 41,  
50520 Bergen, Norway

November 22, 2016

We analyze an optimized artificial fixed-stress iteration scheme for the numerical approximation of the Biot system modelling fluid flow in deformable porous media. The iteration is based on a prescribed constant artificial volumetric mean total stress in the first half step. The optimization comes through the adaptation of a numerical stabilization or tuning parameter and aims at an acceleration of the iterations. The separated subproblems of fluid flow, written as a mixed first order in space system, and mechanical deformation are discretized by space-time finite element methods of arbitrary order. Continuous and discontinuous discretizations of the time variable are encountered. The convergence of the iteration schemes is proved for the continuous and fully discrete case. The choice of the optimization parameter is identified in the proofs of convergence of the iterations. The analyses are illustrated and confirmed by numerical experiments.

**Keywords.** Deformable porous media, fixed-stress iterative coupling, space-time finite element methods, variational time discretization

## 1 Introduction and mathematical model

Many physical and technical problems in mechanical, environmental and petroleum engineering as well as in biomechanics and biomedicine involve interactions between flow and mechanical deformation in porous media. Therefore, the ability to simulate coupled mechanical deformations and fluid flow in such media is of particular importance from the point of view of physical realism. Numerical modelling of such coupled processes is complex due to the structure of the equations and continues to remain a challenging task.

---

\*bause@hsu-hh.de (corresponding author), <sup>†</sup>florin.radu@uib.no, <sup>‡</sup>koecher@hsu-hh.de

We consider modelling flow in deformable porous media by the quasi-static Biot system [26],

$$-\nabla \cdot \boldsymbol{\sigma}(\mathbf{u}, p) = \rho_b \mathbf{g}, \quad (1.1)$$

$$\partial_t \left( \frac{1}{M} p + \nabla \cdot (b\mathbf{u}) \right) + \nabla \cdot \mathbf{q} = f, \quad \mathbf{q} = -\frac{\mathbf{K}}{\eta} (\nabla p - \rho_f \mathbf{g}), \quad (1.2)$$

$$p(0) = p_0, \quad \mathbf{u}(0) = \mathbf{0}, \quad (1.3)$$

with supplemented boundary conditions and the total stress  $\boldsymbol{\sigma}(\mathbf{u}, p) = \boldsymbol{\sigma}_0 + \mathbf{C} : \boldsymbol{\varepsilon}(\mathbf{u}) - b(p - p_0)\mathbf{I}$ , to be satisfied in the bounded Lipschitz domain  $\Omega \subset \mathbb{R}^d$ , with  $d = 2$  or  $d = 3$ , and for the time  $t \in I = (0, T]$ . In (1.1)–(1.3), we denote by  $\mathbf{u}$  the unknown displacement field,  $p$  the unknown fluid pressure,  $\boldsymbol{\varepsilon}(\mathbf{u}) = (\nabla \mathbf{u} + (\nabla \mathbf{u})^\top)/2$  the linearized strain tensor,  $\mathbf{C}$  the Gassmann rank-4 tensor of elasticity,  $\boldsymbol{\sigma}_0$  the reference state stress tensor,  $b$  Biot’s coefficient,  $\rho_b = \phi \rho_f + (1 - \phi)\rho_s$  the bulk density with porosity  $\phi$  and fluid and solid phase density  $\rho_f$  and  $\rho_s$ ,  $p_0$  the reference state fluid pressure,  $M$  Biot’s modulus and, finally, by  $\mathbf{q}$  Darcy’s velocity or the fluid flux. Eq. (1.1) models conservation of momentum and the first of the equations (1.2) describes conservation of mass. The second of the equations (1.2) is the well-known Darcy law with permeability field  $\mathbf{K}$  and fluid viscosity  $\eta$ . Further,  $\mathbf{g}$  denotes gravity or, in general, some body force and  $f$  is a volumetric source. The quantities  $\eta$ ,  $M$ ,  $\rho_f$  and  $\rho_s$  are positive constants. The matrix  $\mathbf{K}$  is supposed to be symmetric and uniformly positive definite. For any symmetric matrix  $\mathbf{B}$  we assume that  $(\mathbf{C}\mathbf{B}) : \mathbf{B} \geq a|\mathbf{B}|^2 + \lambda \text{tr}(\mathbf{B})^2$  is satisfied with some constant  $a > 0$  and the drained bulk modulus  $\lambda$ ; cf. [28]. We assume that  $\rho_b$  is independent of time and that  $\rho_b \mathbf{g} = -\nabla \cdot \boldsymbol{\sigma}_0$ . Here, the quasi-static feature is due to the negligence of the solid’s acceleration in problem (1.1) of mechanical deformation. This prevents the applicability of the model (1.1)–(1.3) to classes of problems for that the contrast coefficients, the ratio between the intrinsic characteristic time and the characteristic time scale of the domain, are not close to the singular limit of vanishing numbers. In [39] an existence, uniqueness and regularity theory is presented for the Biot system (1.1)–(1.3) in a Hilbert space setting. In [40] the well-posedness is shown for a wider class of diffusion problems in poro-elastic media with more general material deformation models.

Iteratively coupled solution methods for the system of (1.1)–(1.3) of coupled fluid flow and mechanical deformation have recently attracted researchers’ interest; cf. [3, 8, 9, 21, 26, 27, 28, 30, 38] and the references therein. Iterative coupling is a sequential approach, in that either the problem of flow or the mechanics is solved first followed by solving the other system using the already calculated information. At each time step this is repeated until a converged solution within a prescribed numerical tolerance is obtained. In [21] it’s shown by an analysis that some of the splitting approaches may exhibit stability problems. Iterative coupling offers the appreciable advantage over the fully coupled method that existing and highly developed discretizations and algebraic solver technology, for instance preconditioning methods, as well as existing software tools can be reused. The construction of efficient preconditioning techniques for solving the arising algebraic systems of equations of fully coupled approaches to poroelasticity has not been satisfactorily solved yet and continues to remain a field of active research [42]. In particular, this applies to the case in that higher order space and time discretization techniques are involved.

In this work we analyze a ”fixed-stress split” type iterative method; cf. [21, 27]. The fixed-stress split iterative method is based on imposing constant volumetric mean total stress  $\sigma_v = \sigma_0 + \lambda \nabla \cdot \mathbf{u} - b(p - p_0)$  in the first half step of fluid flow. In our approach we use some optimized fixed-stress split by prescribing a constant artificial volumetric mean total stress that is given

for  $\sigma_0 = 0$  and  $p_0 = 0$  by  $\sigma_v = \lambda \nabla \cdot \mathbf{u} - L \lambda b^{-1} p$  with some additional numerical parameter  $L > 0$  that has to be tuned to accelerate the iteration procedure and to reduce the numbers of iterations that are required for the adherence of a prescribed numerical tolerance. In contrast to [27], a mixed formulation of the flow problem (1.2) is considered here. In this paper we prove the convergence of the proposed iteration scheme by a fixed point argument and identify an optimal choice for the numerical parameter  $L$ . This is done for the continuous case of the iteratively coupled subproblems of partial differential equations and for the fully discrete case of space-time finite approximations of the subproblems. Our analysis yields the same choice for the numerical parameter  $L$  for the either cases, even though completely different techniques of proof are used. Therefore, the acceleration of the iteration's convergence is not impacted by the time or space step size or the polynomial degree of the finite element methods in time and space. Our numerical tests nicely confirm the choice of the acceleration parameter  $L$  that is suggested by our numerical analysis of the schemes. The numerical results show that the number of required iterations can strongly be reduced by using the proposed optimized fixed-stress split iterative method along with the suggested choice of the tuning parameter  $L$ .

For the numerical approximation of the separated subproblems of fluid flow and mechanical deformation we use space-time finite element methods. Continuous and discontinuous finite element discretizations of the time variable are studied. For the spatial discretization of the flow problem mixed finite element methods (cf. [10]) ensuring local mass conservation and an inherent approximation of the flux variable are used. Due to these properties, mixed finite element methods have shown in numerous works their superiority over standard conforming methods for the numerical simulation of fluid flow in porous media; cf. [19] for its application to reservoir geomechanics. For the spatial discretization of the displacement variable a standard conforming approach is used in order to simplify the analysis. In the future we will use discontinuous Galerkin methods for the discretization of the displacement field and the approximation of the subproblem of mechanical deformation since we expect from our former works (cf. [22, 23]) on discontinuous Galerkin methods significant advantages for future generalizations of the underlying Biot model, for instance, to the Biot–Allard system [26]. Moreover, the discontinuous Galerkin discretization of the displacement variable helps to avoid locking phenomena. For a discussion of locking phenomena arising in poroelasticity and remedies we refer to [24, 29, 31, 32, 36] and the references therein.

Since recently, variational time discretization schemes based on continuous or discontinuous finite element techniques have been developed to the point that they can be put into use (cf., e.g., [1, 2, 6, 13, 18, 17, 23, 15] and the references therein) and demonstrated their significant advantages. Higher order methods are naturally embedded in these schemes and the uniform variational approach simplifies stability and error analyses. Further, goal-oriented error control [4] based on the dual weighted residual approach relies on variational space-time formulations and the concepts of adaptive finite element techniques for changing the polynomial degree as well as the length of the time intervals become applicable. However, in the context of numerical modelling flow in porous or deformable media higher order space-time finite element methods or even only higher order time discretizations have rarely been used in practice so far. However, for applications with strong fluctuations of physical quantities and involved highly dynamical processes, for instance in vibro acoustics and reactive multicomponent and multiphase subsurface flow, as well as for future generalizations to more complex models like the Biot–Allard system [26] the needfulness of developing and analyzing higher order techniques is evident.

The paper is organized as follows. In Sec. 2 we introduce the iterative coupling scheme of

subproblems of partial differential equations for fluid flow and mechanical deformation and prove its convergence. In Sec. 3 the space-time finite element discretization of the subproblems is introduced for a continuous and a discontinuous approximation of the time variable. In Sec. 4 we then prove convergence of the iterations for both families of space-time finite element approximations. Sec. 5 illustrates the given analyses by numerical computations and confirms our theoretical observations. Sec. 6 summarizes the results of this work.

Throughout the paper, our notation is standard. We denote by  $H^m(\Omega)$  the Sobolev space of  $L^2$  functions with derivatives up to order  $m$  in  $L^2(\Omega)$ . By  $\langle \cdot, \cdot \rangle$  and  $\|\cdot\|$  denote the inner product and norm in  $L^2(\Omega)$ , respectively, where we do not differ in the notation between inner products and norms of scalar- and vector-valued functions. For rank-2 tensors  $\mathbf{A}, \mathbf{B} \in \mathbb{R}^{d,d}$  we use the notation  $\langle \mathbf{A}, \mathbf{B} \rangle = \int_{\Omega} \sum_{i,j=1}^d A_{ij} B_{ij} \, d\mathbf{x}$ . Further, let  $H_0^1(\Omega) = \{u \in H^1(\Omega) \mid u = 0 \text{ on } \partial\Omega\}$ . For the mixed problem formulation of the flow problem (1.2) we put

$$\mathbf{V} = \mathbf{H}(\text{div}; \Omega), \quad W = L^2(\Omega),$$

where  $\mathbf{H}(\text{div}; \Omega) = \{\mathbf{q} \in \mathbf{L}^2(\Omega) \mid \nabla \cdot \mathbf{q} \in L^2(\Omega)\}$ . Let  $X_0 \subset X \subset X_1$  be three reflexive Banach spaces with continuous embeddings. Then we consider the following set of spaces,

$$\begin{aligned} C(\bar{I}; X) &= \{w : [0, T] \rightarrow X \mid w \text{ is continuous}\}, \\ L^2(I; X) &= \left\{ w : (0, T) \rightarrow X \mid \int_0^T \|w(t)\|_X^2 \, dt < \infty \right\}, \\ H^1(I; X_0, X_1) &= \{w \in L^2(I; X_0) \mid \partial_t w \in L^2(I; X_1)\}, \end{aligned}$$

that are equipped with their natural norms (cf. [14]) and where the time derivative  $\partial_t$  is understood in the sense of distributions on  $(0, T)$ . In particular, every function in  $H^1(I; X_0, X_1)$  is continuous on  $[0, T]$  with values in  $X$ ; cf. [14]. For  $X_0 = X = X_1$  we simply write  $H^1(I; X)$ .

## 2 Iterative coupling scheme and proof of convergence

In this section we introduce our iterative coupling scheme of subproblems of partial differential equations and prove its convergence. The fully discrete counterpart of the scheme and its convergence is treated below in Sec. 3 and 4, respectively. In our analysis of the scheme we restrict ourselves to homogeneous Dirichlet boundary conditions. In our numerical experiments (cf. Section 5) more general boundary conditions are also encountered. Without loss of generality, we assume vanishing initial conditions  $p_0 = 0$  and  $\mathbf{u}_0 = \mathbf{0}$ . We put  $\boldsymbol{\sigma}_0 = \mathbf{0}$  and assume that  $\mathbf{g}(0) = \mathbf{0}$ . Further, we prescribe an isotropic material behavior such that the Gassmann rank-4 tensor of elasticity  $\mathbf{C}$  is given by  $c_{ijkl} = \lambda \delta_{ij} \delta_{kl} + \mu (\delta_{ik} \delta_{jl} + \delta_{il} \delta_{jk})$  and the total stress reads as  $\boldsymbol{\sigma}(\mathbf{u}, p) = 2\mu \boldsymbol{\varepsilon}(\mathbf{u}) + \lambda \nabla \cdot \mathbf{u} \mathbf{I} - b p \mathbf{I}$  with  $\mu > 0$  and  $\lambda$  denoting the Lamé parameters. We let  $\lambda > 0$  which is satisfied for most of the materials. These assumptions can be relaxed further to study more complex and non isotropic material behavior. To simplify the notation, we write  $\mathbf{K}$  instead of  $\mathbf{K}/\eta$  and add the gravity term of (1.2) to the right-hand side term  $f$ . Under these assumptions Eqs. (1.1)–(1.3) read as

$$-\nabla \cdot (2\mu \boldsymbol{\varepsilon}(\mathbf{u}) + \lambda \nabla \cdot \mathbf{u} \mathbf{I} - b p \mathbf{I}) = \rho_b \mathbf{g}, \quad (2.1)$$

$$\partial_t \left( \frac{1}{M} p + \nabla \cdot (b \mathbf{u}) \right) + \nabla \cdot \mathbf{q} = f, \quad \mathbf{q} = -\mathbf{K} \nabla p, \quad (2.2)$$

$$p(0) = 0, \quad \mathbf{u}(0) = \mathbf{0} \quad (2.3)$$

for  $\mathbf{x} \in \Omega$  and  $t \in I$  with the boundary conditions

$$p = 0 \quad \text{and} \quad \mathbf{u} = \mathbf{0} \quad \text{on } \partial\Omega \times I. \quad (2.4)$$

For the data  $\mathbf{g}$ ,  $f$  and  $\mathbf{K}$  we assume at first that the conditions  $\mathbf{g} \in L^2(I; \mathbf{L}^2(\Omega))$ ,  $f \in L^2(I; L^2(\Omega))$  and  $\mathbf{K} \in \mathbf{L}^\infty(\Omega)$  are satisfied.

For  $\Omega = (0, l)^d$  and under periodic boundary conditions for  $\mathbf{u}$  and  $p$  with period  $l$  and for smooth  $l$ -periodic functions  $p_0$ ,  $f$  and  $\boldsymbol{\sigma}_0$  it is shown in [26] that the system (1.1)–(1.3) admits a unique periodic solution  $\{\mathbf{u}, p\} \in C(\bar{I}; \mathbf{H}_{\text{per}}^1(\Omega) \cap \mathbf{L}_0^2(\Omega)) \times H^1(\Omega \times I) \cap C(\bar{I}; H_{\text{per}}^1(\Omega))$ . Further, for  $\mathbf{g} \in C_0^\infty(\mathbb{R}^+; \mathbf{L}_0^2(\Omega))$  and homogeneous initial conditions the solution of the system is smooth in time with  $\{\mathbf{u}, p\} \in H^k(I; \mathbf{H}_{\text{per}}^1(\Omega)) \times H^k(I; H_{\text{per}}^1(\Omega))$ , for all  $k \in \mathbb{N}$ ; cf. [26].

To solve the equations (2.1)–(2.4) we use a *fixed-stress iterative splitting scheme*; cf. [27]. This scheme consists in imposing a constant artificial volumetric mean total stress  $\sigma_v = \lambda \nabla \cdot \mathbf{u} - L \lambda b^{-1} p$  in the first half step. Here, the parameter  $L > 0$  is a free to be chosen constant that is specified below. The supplement "artificial", that is used here, is due to the additional parameter  $L$  in contrast to the proper definition of the volumetric mean total stress given by  $\sigma_v = \lambda \nabla \cdot \mathbf{u} - b p$ . By adding the parameter  $L$  we aim to find an iteration scheme with smaller and optimal contraction number compared to the standard definition of  $\sigma_v$ ; cf. [27]. Supposing a constant artificial volumetric mean total stress then yields in the first half step of fluid flow

$$\left(\frac{1}{M} + L\right) \partial_t p^{k+1} + \nabla \cdot \mathbf{q}^{k+1} = f - b \nabla \cdot \partial_t \mathbf{u}^k + L \partial_t p^k, \quad \mathbf{q}^{k+1} = -\mathbf{K} \nabla p^{k+1} \quad (2.5)$$

on  $\Omega \times I$ ,  $p^{k+1}(0) = 0$  in  $\Omega$  and  $p^{k+1} = 0$  on  $\partial\Omega \times I$ . In each iteration step problem (2.5) of fluid flow is thus decoupled from the mechanical deformation subproblem and can be solved independently. In the second half step the effective deformation is then obtained by solving

$$-\nabla \cdot \left(2\mu \boldsymbol{\varepsilon}(\mathbf{u}^{k+1}) + \lambda \nabla \cdot \mathbf{u}^{k+1} \mathbf{I}\right) = \rho_b \mathbf{g} - b \nabla p^{k+1} \quad (2.6)$$

on  $\Omega \times I$ , where  $\mathbf{u}^{k+1}(0) = \mathbf{0}$  and  $\mathbf{u}^{k+1} = 0$  on  $\partial\Omega \times I$ .

The weak formulation of problem (2.5) in the space-time framework then reads as follows: Let  $\tilde{f}^k := f - b \nabla \cdot \partial_t \mathbf{u}^k + L \partial_t p^k$  with  $\tilde{f}^k \in L^2(I; W)$  be given. Find  $p^{k+1} \in H^1(I; W)$  and  $\mathbf{q}^{k+1} \in L^2(I; \mathbf{V})$  such that  $p^{k+1}(0) = 0$  and

$$\left(\frac{1}{M} + L\right) \int_I \langle \partial_t p^{k+1}, w \rangle dt + \int_I \langle \nabla \cdot \mathbf{q}^{k+1}, w \rangle dt = \int_I \langle \tilde{f}^k, w \rangle dt, \quad (2.7)$$

$$\int_I \langle \mathbf{K}^{-1} \mathbf{q}^{k+1}, \mathbf{v} \rangle dt - \int_I \langle p^{k+1}, \nabla \cdot \mathbf{v} \rangle dt = 0 \quad (2.8)$$

for all  $w \in L^2(I; W)$  and  $\mathbf{v} \in L^2(I; \mathbf{V})$ .

The weak form of problem (2.6) reads as follows: Let  $p^{k+1} \in H^1(I; W)$  be given. Find  $\mathbf{u}^{k+1} \in H^1(I; \mathbf{H}^1(\Omega)) \cap L^2(I; \mathbf{H}_0^1(\Omega))$  such that  $\mathbf{u}(0) = \mathbf{0}$  and

$$\begin{aligned} \int_I 2\mu \langle \boldsymbol{\varepsilon}(\mathbf{u}^{k+1}), \boldsymbol{\varepsilon}(\mathbf{z}) \rangle dt + \int_I \lambda \langle \nabla \cdot \mathbf{u}^{k+1}, \nabla \cdot \mathbf{z} \rangle dt \\ = \rho_b \int_I \langle \mathbf{g}, \mathbf{z} \rangle dt + b \int_I \langle p^{k+1} \mathbf{I}, \boldsymbol{\varepsilon}(\mathbf{z}) \rangle dt \end{aligned} \quad (2.9)$$

for all  $\mathbf{z} \in L^2(I; \mathbf{H}_0^1(\Omega))$ .

To simplify the notation, we put

$$\begin{aligned}\mathcal{W} &= \{w \in H^1(I; H^1(\Omega)) \mid w \in C(\bar{I}; H_0^1(\Omega))\}, \\ \mathcal{V} &= \{\mathbf{v} \in L^2(I; \mathbf{V}) \mid \mathbf{v} \in C(\bar{I}; \mathbf{L}^2(\Omega))\}, \\ \mathcal{Z} &= \{\mathbf{z} \in H^1(I; \mathbf{H}^1(\Omega)) \mid \mathbf{z} \in C(\bar{I}; \mathbf{H}_0^1(\Omega)), \partial_t \mathbf{u} \in L^2(I; \mathbf{H}^2(\Omega))\}.\end{aligned}$$

The following theorem shows the convergence of the iteration scheme (2.7) to (2.9). In contrast to [27] our proof is based on a mixed formulation of the flow problem. Moreover, the proof is presented explicitly here in order to show that the convergence proofs for the iteration scheme on the continuous and discrete level lead to the same optimal parameter  $L$ , even though completely different techniques of proof are used.

**Theorem 2.1** *Suppose that  $\partial\Omega$  and the permeability field  $\mathbf{K}$  are sufficiently regular. Let  $f \in L^2(I; H^1(\Omega))$  and  $\mathbf{g} \in H^1(I; \mathbf{L}^2(\Omega))$  be satisfied. Then, for any  $L \geq b^2/(2\lambda)$  the operator  $\mathcal{S} : (p^k, \mathbf{q}^k, \mathbf{u}^k) \mapsto (p^{k+1}, \mathbf{q}^{k+1}, \mathbf{u}^{k+1})$  maps  $\mathcal{D} = \{(p, \mathbf{q}, \mathbf{u}) \in \mathcal{W} \times \mathcal{V} \times \mathcal{Z} \mid p(0) = 0, \mathbf{u}(0) = \mathbf{0}\}$  into itself and is a contraction mapping on  $\mathcal{D}$ . Therefore, the operator  $\mathcal{S}$  has a unique fixed point in  $\mathcal{D}$ . The contraction constant is smallest for  $L = b^2/(2\lambda)$  with value  $LM/(LM + 1)$ .*

**Proof.** Firstly, we show that  $\mathcal{S}$  maps  $\mathcal{D}$  into itself. For this, let  $\{p^k, \mathbf{q}^k, \mathbf{u}^k\} \in \mathcal{W} \times \mathcal{V} \times \mathcal{Z}$  be given. Under the assumptions of the theorem it follows that

$$\tilde{f}^k \in L^2(I; H^1(\Omega)) \quad \text{for} \quad \tilde{f}^k = f - b \nabla \cdot \partial_t \mathbf{u}^k + L \partial_t p^k.$$

The variational problem (2.7), (2.8) then admits a unique solution  $p^{k+1} \in \mathcal{W}$  and  $\mathbf{q}^{k+1} \in \mathcal{V}$ . This directly follows from parabolic regularity theory; cf., e.g., [16]. For  $p^{k+1} \in H^1(I; H^1(\Omega))$  the second of the right-hand side terms in Eq. (2.9) can be rewritten as

$$\int_I \langle p^{k+1} \mathbf{I}, \boldsymbol{\varepsilon}(\mathbf{z}) \rangle \, d\tau = \int_I \langle \nabla p^{k+1}, \mathbf{z} \rangle \, d\tau.$$

By means of elliptic regularity theory the variational problem (2.9) then admits a unique solution  $\mathbf{u}^{k+1} \in \mathcal{Z}$ ; cf., e.g., [11]. We note that  $p^{k+1} \in \mathcal{W}$ ,  $\mathbf{q}^{k+1} \in \mathcal{V}$  and  $\mathbf{u}^{k+1} \in \mathcal{Z}$  are even strong solutions of the problems (2.5) and (2.6), respectively.

Secondly, we now show that the operator  $\mathcal{S}$  is a contraction mapping on  $\mathcal{D}$ . With

$$\sigma_v = \lambda \nabla \cdot \mathbf{u} - \frac{L\lambda}{b} p \tag{2.10}$$

and  $S_p^{k+1} = p^{k+1} - p^k$ ,  $S_q^{k+1} = \mathbf{q}^{k+1} - \mathbf{q}^k$ ,  $S_u^{k+1} = \mathbf{u}^{k+1} - \mathbf{u}^k$ ,  $S_{\sigma_v}^k = \sigma_v^k - \sigma_v^{k-1}$  for the differences of the iterates we get from the first of the equations (2.7) that

$$\left(\frac{1}{M} + L\right) \int_0^t \langle \partial_t S_p^{k+1}, w \rangle \, d\tau + \int_0^t \langle \nabla \cdot S_q^{k+1}, w \rangle \, d\tau = - \int_0^t \frac{b}{\lambda} \langle \partial_t S_{\sigma_v}^k, w \rangle \, d\tau \tag{2.11}$$

for all  $w \in L^2(I; W)$ . Choosing  $w = S_p^{k+1}$  in Eq. (2.11) and using the inequalities of Cauchy–

Schwarz and Cauchy–Young we obtain that

$$\begin{aligned}
& \left( \frac{1}{M} + L \right) \frac{b^2}{L^2 \lambda^2} \int_0^t \int_{\Omega} \left| \frac{L\lambda}{b} \partial_t S_p^{k+1} \right|^2 d\mathbf{x} d\tau + \int_0^t \langle \nabla \cdot \mathbf{S}_q^{k+1}, \partial_t S_p^{k+1} \rangle d\tau \\
&= - \int_0^t \frac{b}{\lambda} \langle \partial_t S_{\sigma_v}^k, \partial_t S_p^{k+1} \rangle d\tau \\
&\leq \frac{\varepsilon}{2} \frac{b^2}{L^2 \lambda^2} \int_0^t \int_{\Omega} \left| \frac{L\lambda}{b} \partial_t S_p^{k+1} \right|^2 d\mathbf{x} d\tau + \frac{b^2}{2\varepsilon \lambda^2} \int_0^t \int_{\Omega} \left| \partial_t S_{\sigma_v}^k \right|^2 d\mathbf{x} d\tau.
\end{aligned}$$

Choosing  $\varepsilon = L + \frac{1}{M}$ , we then get that

$$\begin{aligned}
& \int_0^t \int_{\Omega} \left| \frac{L\lambda}{b} \partial_t S_p^{k+1} \right|^2 d\mathbf{x} d\tau + \gamma \int_0^t \langle \nabla \cdot \mathbf{S}_q^{k+1}, \partial_t S_p^{k+1} \rangle d\tau \\
&\leq \left( \frac{L}{L + 1/M} \right)^2 \int_0^t \int_{\Omega} \left| \partial_t S_{\sigma_v}^k \right|^2 d\mathbf{x} d\tau
\end{aligned} \tag{2.12}$$

with  $\gamma = \frac{2L^2 \lambda^2}{b^2} \cdot \frac{1}{L + \frac{1}{M}} > 0$ .

Next, taking the time derivative of the second of the equations (2.5) and testing the resulting identity with  $\mathbf{v} = \mathbf{S}_q^{k+1}$ , we have that

$$\int_0^t \langle \mathbf{K}^{-1} \partial_t \mathbf{S}_q^{k+1}, \mathbf{S}_q^{k+1} \rangle d\tau - \int_0^t \langle \nabla \cdot \mathbf{S}_q^{k+1}, \partial_t S_p^{k+1} \rangle d\tau = 0.$$

By means of  $\frac{1}{2} \frac{d}{d\tau} \langle a, a \rangle = \langle \partial_t a, a \rangle$  we conclude from the previous equation that

$$\begin{aligned}
& \int_0^t \langle \nabla \cdot \mathbf{S}_q^{k+1}, \partial_t S_p^{k+1} \rangle d\tau = \int_0^t \frac{1}{2} \frac{d}{d\tau} \langle \mathbf{K}^{-1} \mathbf{S}_q^{k+1}, \mathbf{S}_q^{k+1} \rangle d\tau \\
&= \frac{1}{2} \langle \mathbf{K}^{-1} \mathbf{S}_q^{k+1}(t), \mathbf{S}_q^{k+1}(t) \rangle - \frac{1}{2} \langle \mathbf{K}^{-1} \mathbf{S}_q^{k+1}(0), \mathbf{S}_q^{k+1}(0) \rangle \\
&= \frac{1}{2} \left\| \mathbf{K}^{-1/2} \mathbf{S}_q^{k+1}(t) \right\|^2.
\end{aligned} \tag{2.13}$$

We note that by definition and Eq. (2.5) along with the regularity conditions of  $\mathcal{D}$  it holds that  $\mathbf{S}_q^{k+1}(0) = -\mathbf{K} \nabla p_0 + \mathbf{K} \nabla p_0 = \mathbf{0}$ .

Finally, taking the time derivative of Eq. (2.6) and testing the resulting equation with  $\mathbf{z} = \partial_t \mathbf{S}_u^{k+1}$  we get that

$$\begin{aligned}
& \frac{2L\lambda^2}{b^2} \int_0^t \int_{\Omega} 2\mu \left| \varepsilon(\partial_t \mathbf{S}_u^{k+1}) \right|^2 d\mathbf{x} d\tau + \frac{2\lambda L \lambda^2}{b^2} \int_0^t \int_{\Omega} \left| \nabla \cdot \partial_t \mathbf{S}_u^{k+1} \right|^2 d\mathbf{x} d\tau \\
&= 2 \int_0^t \left\langle \frac{L\lambda}{b} \partial_t S_p^{k+1}, \lambda \nabla \cdot (\partial_t \mathbf{S}_u^{k+1}) \right\rangle d\tau.
\end{aligned} \tag{2.14}$$

Applying the algebraic identity

$$2\langle a, b \rangle = \langle a, a \rangle + \langle b, b \rangle - \langle a - b, a - b \rangle$$

to the right-hand side of Eq. (2.14) and recalling definition (2.10) we find that

$$\begin{aligned}
& \frac{2L\lambda^2}{b^2} \int_0^t \int_{\Omega} 2\mu \left| \varepsilon(\partial_t \mathbf{S}_u^{k+1}) \right|^2 d\mathbf{x} d\tau + \frac{2\lambda L}{b^2} \int_0^t \int_{\Omega} \left| \lambda \nabla \cdot \partial_t \mathbf{S}_u^{k+1} \right|^2 d\mathbf{x} d\tau \\
&= \int_0^t \int_{\Omega} \left| \frac{L\lambda}{b} \partial_t \mathbf{S}_p^{k+1} \right|^2 d\mathbf{x} d\tau + \int_0^t \int_{\Omega} \left| \lambda \nabla \cdot \partial_t \mathbf{S}_u^{k+1} \right|^2 d\mathbf{x} d\tau \\
&\quad - \int_0^t \int_{\Omega} \left| \partial_t \mathbf{S}_{\sigma_v}^{k+1} \right|^2 d\mathbf{x} d\tau.
\end{aligned} \tag{2.15}$$

Finally, summing up the relations (2.12), (2.13) and (2.15) yields that

$$\begin{aligned}
& \int_0^t \int_{\Omega} \left| \partial_t \mathbf{S}_{\sigma_v}^{k+1} \right|^2 d\mathbf{x} dt + \frac{2L\lambda^2}{b^2} \int_0^t \int_{\Omega} 2\mu \left| \varepsilon(\partial_t \mathbf{S}_u^{k+1}) \right|^2 d\mathbf{x} d\tau \\
&\quad + \left( \frac{2\lambda L}{b^2} - 1 \right) \int_0^t \int_{\Omega} \left| \lambda \nabla \cdot \partial_t \mathbf{S}_u^{k+1} \right|^2 d\mathbf{x} d\tau + \frac{\gamma}{2} \left\| \mathbf{K}^{-1/2} \mathbf{S}_q^{k+1}(t) \right\|^2 \\
&\leq \left( \frac{L}{L+1/M} \right)^2 \int_0^t \int_{\Omega} \left| \partial_t \mathbf{S}_{\sigma_v}^k \right|^2 d\mathbf{x} d\tau.
\end{aligned} \tag{2.16}$$

Inequality (2.16) yields a contraction map only if  $L \geq b^2/(2\lambda)$ . The contraction constant is smallest for  $L = b^2/(2\lambda)$ .

On the space  $\mathcal{D}$  the expression on the left-hand side of (2.16) defines a metric by

$$\begin{aligned}
& d_{\mathcal{D}} \left( (\mathbf{u}, p, \mathbf{q}), (\mathbf{0}, 0, \mathbf{0}) \right) \\
&= \frac{4L\lambda^2\mu}{b^2} \left\| \varepsilon(\partial_t \mathbf{u}) \right\|_{L^2(\Omega \times I)}^2 + \left( \frac{2\lambda L}{b^2} - 1 \right) \left\| \lambda \nabla \cdot \partial_t \mathbf{u} \right\|_{L^2(\Omega \times I)}^2 \\
&\quad + \left\| \partial_t \left( \lambda \nabla \cdot \mathbf{u} - \frac{L\lambda}{b} p \right) \right\|_{L^2(\Omega \times I)}^2 + \frac{\gamma}{2} \max_{0 \leq t \leq T} \left\| \mathbf{K}^{-1/2} \mathbf{q}(t) \right\|_{L^2(\Omega)}^2.
\end{aligned}$$

Summarizing the previous steps, we note that the operator  $\mathcal{S}$  maps  $\mathcal{D}$  into itself and, by inequality (2.16), satisfies

$$d_{\mathcal{D}} \left( (\mathbf{u}^{k+1}, p^{k+1}, \mathbf{q}^{k+1}) - (\mathbf{u}^k, p^k, \mathbf{q}^k) \right) \leq \delta d_{\mathcal{D}} \left( (\mathbf{u}^k, p^k, \mathbf{q}^k) - (\mathbf{u}^{k-1}, p^{k-1}, \mathbf{q}^{k-1}) \right)$$

with  $\delta = \frac{L}{L+1/M}$ . Therefore, the operator  $\mathcal{S}$  is a contraction mapping and by the contraction mapping principle, it has a unique fixed point.  $\blacksquare$

### 3 Space-time discretization

In this section we introduce our space time finite approximation of the subproblems (2.7), (2.8) and (2.9) of fluid flow and mechanical deformation by space-time finite element techniques. For the discretization of the time variable we consider using continuous and discontinuous finite element methods. For the spatial discretization of the subproblem of fluid flow mixed



finite element techniques are applied. Standard conforming finite element methods are used for the spatial discretization of the subproblem of mechanical deformation. The derivation of the discrete systems is done briefly here. For the application of space-time finite element methods to the subproblems of our iteration scheme and the derivation of their algebraic formulations as well as for the construction of appropriate iterative linear solvers and preconditioning techniques we refer to [6, 23].

We decompose the time interval  $(0, T]$  into  $N$  subintervals  $I_n = (t_{n-1}, t_n]$ , where  $n \in \{1, \dots, N\}$  and  $0 = t_0 < t_1 < \dots < t_{n-1} < t_n = T$  and  $\tau = \max_{n=1, \dots, N} (t_n - t_{n-1})$ . Further we denote by  $\mathcal{T}_h = \{K\}$  a finite element decomposition of mesh size  $h$  of the polyhedral domain  $\bar{\Omega}$  into closed subsets  $K$ , quadrilaterals in two dimensions and hexahedrons in three dimensions. For the spatial discretization of (2.5) we use a mixed finite element approach. We choose the class of Raviart–Thomas elements for the two-dimensional case and the class of Raviart–Thomas–Nédélec elements in three space dimensions, where  $W_h^s \subset L^2(\Omega)$  with  $\mathbf{W}_h^s = \{w_h \in L^2(\Omega) \mid w_h|_K \circ T_K \in \mathbb{Q}_s\}$  and  $\mathbf{V}_h^s \subset \mathbf{H}(\text{div}; \Omega)$  denote the corresponding inf-sup stable pair of finite element spaces; cf. [6, 10, 34] for the exact definition of  $\mathbf{V}_h^s$ . Here,  $\mathbb{Q}_s$  is the space of polynomials that are of degree less than or equal to  $s$  with respect to each variable  $x_1, \dots, x_d$  and  $T_K$  is a suitable invertible mapping of the reference cube  $\hat{K}$  to the element  $K$  of the triangulation  $\mathcal{T}_h$ . For the spatial approximation of the displacement field  $\mathbf{u}$  of (2.6) we discretize the space variables by means of a conforming Galerkin method with finite element space  $\mathbf{H}_h^l = \{\mathbf{z}_h \in C(\bar{\Omega}) \mid \mathbf{z}_h|_K \circ T_K \in \mathbb{Q}_l^d, \mathbf{z}_h|_{\partial\Omega} = \mathbf{0}\}$ . The fully discrete space-time finite element spaces of functions that are continuous in time are then given by

$$\mathcal{W}_{\tau,h}^{r,s} = \{w_{\tau,h} \in C(\bar{I}; L^2(\Omega)) \mid w_{\tau,h}|_{I_n} \in \mathcal{P}_r(I_n; W_h^s)\}, \quad (3.1)$$

$$\mathcal{V}_{\tau,h}^{r,s} = \{\mathbf{v}_{\tau,h} \in C(\bar{I}; \mathbf{H}(\text{div}; \Omega)) \mid \mathbf{v}_{\tau,h}|_{I_n} \in \mathcal{P}_r(I_n; \mathbf{V}_h^s)\}, \quad (3.2)$$

$$\mathcal{Z}_{\tau,h}^{r,l} = \{\mathbf{z}_{\tau,h} \in C(\bar{I}; \mathbf{H}_0^1(\Omega)) \mid \mathbf{z}_{\tau,h}|_{I_n} \in \mathcal{P}_r(I_n; \mathbf{H}_h^l)\}, \quad (3.3)$$

where  $\mathcal{P}_r(I_n; X)$  denotes the space of all polynomials in time up to degree  $r \geq 0$  on  $I_n$  with values in  $X$ . We choose  $l = s+1$  to equilibrate the convergence rates of the spatial discretization for the three unknowns  $p, \mathbf{q}$  and  $\mathbf{u}$ ; cf. [30, Part I, Thm. 5.2]. For short, we will also use the abbreviations  $W_h = W_h^s$ ,  $\mathbf{V}_h = \mathbf{V}_h^s$  and  $\mathbf{H}_h = \mathbf{H}_h^{s+1}$  in the sequel.

Discontinuous counterparts  $\widetilde{\mathcal{W}}_{\tau,h}^{r,s}$ ,  $\widetilde{\mathcal{V}}_{\tau,h}^{r,s}$  and  $\widetilde{\mathcal{H}}_{\tau,h}^{r,l}$  of the spaces (3.1)–(3.3), consisting of functions not necessarily being continuous in time, are then defined by

$$\widetilde{\mathcal{W}}_{\tau,h}^{r,s} = \{w_{\tau,h} \in L^2(I; L^2(\Omega)) \mid w_{\tau,h}|_{I_n} \in \mathcal{P}_r(I_n; W_h^s), w_{\tau,h}(0) \in W_h^s\}, \quad (3.4)$$

$$\widetilde{\mathcal{V}}_{\tau,h}^{r,s} = \{\mathbf{v}_{\tau,h} \in L^2(I; \mathbf{H}(\text{div}; \Omega)) \mid \mathbf{v}_{\tau,h}|_{I_n} \in \mathcal{P}_r(I_n; \mathbf{V}_h^s), \mathbf{v}_{\tau,h}(0) \in \mathbf{V}_h^s\}, \quad (3.5)$$

$$\widetilde{\mathcal{Z}}_{\tau,h}^{r,l} = \{\mathbf{z}_{\tau,h} \in L^2(I; \mathbf{H}_0^1(\Omega)) \mid \mathbf{z}_{\tau,h}|_{I_n} \in \mathcal{P}_r(I_n; \mathbf{H}_h^l), \mathbf{z}_{\tau,h}(0) \in \mathbf{H}_h^l\}. \quad (3.6)$$

### 3.1 The cGP( $r$ )–MFEM( $s$ )cG( $s+1$ ) approach.

The space-time finite element approximation of the flow problem (2.7), (2.8) by a continuous finite element approach in time reads as follows: Let  $\mathbf{u}_{\tau,h}^k \in \mathcal{Z}_{\tau,h}^{r,s+1}$ ,  $p_{\tau,h}^k \in \mathcal{W}_{\tau,h}^{r,s}$  be given and

$$l_p^k(\mathbf{w}_{\tau,h}) = \left\langle f - b \nabla \cdot \partial_t \mathbf{u}_{\tau,h}^k + L \partial_t p_{\tau,h}^k, w_{\tau,h} \right\rangle,$$

for  $w_{\tau,h} \in \widetilde{\mathcal{W}}_{\tau,h}^{r-1,s}$ . Find  $p_{\tau,h}^{k+1} \in \mathcal{W}_{\tau,h}^{r,s}$  and  $\mathbf{q}_{\tau,h}^{k+1} \in \mathcal{V}_{\tau,h}^{r,s}$  with  $p_{\tau,h}^{k+1}(0) = 0$  such that

$$\sum_{n=1}^N \left\{ \int_{t_{n-1}}^{t_n} \left( \frac{1}{M} + L \right) \langle \partial_t p_{\tau,h}^{k+1}, w_{\tau,h} \rangle dt + \int_{t_{n-1}}^{t_n} \langle \nabla \cdot \mathbf{q}_{\tau,h}^{k+1}, w_{\tau,h} \rangle dt \right\} = \sum_{n=1}^N \int_{t_{n-1}}^{t_n} l_p^k(w_{\tau,h}) dt, \quad (3.7)$$

$$\sum_{n=1}^N \left\{ \int_{t_{n-1}}^{t_n} \langle \mathbf{K}^{-1} \mathbf{q}_{\tau,h}^{k+1}, \mathbf{v}_{\tau,h} \rangle dt - \int_{t_{n-1}}^{t_n} \langle p_{\tau,h}^{k+1}, \nabla \cdot \mathbf{v}_{\tau,h} \rangle dt \right\} = 0 \quad (3.8)$$

for all  $w_{\tau,h} \in \widetilde{\mathcal{W}}_{\tau,h}^{r-1,s}$  and  $\mathbf{s}_{\tau,h} \in \widetilde{\mathcal{V}}_{\tau,h}^{r-1,s}$ .

The corresponding space-time finite element approximation of the problem (2.9) of mechanical deformation reads as follows: Let  $p_{\tau,h}^{k+1} \in \mathcal{W}_{\tau,h}^{r,s}$  be given and

$$l_{\mathbf{u}}^{k+1}(\mathbf{z}_{\tau,h}) = b \langle p_{\tau,h}^{k+1}, \nabla \cdot \mathbf{z}_{\tau,h} \rangle$$

for  $\mathbf{z}_{\tau,h} \in \widetilde{\mathcal{Z}}_{\tau,h}^{r,s+1}$ . Find  $\mathbf{u}_{\tau,h}^{k+1} \in \mathcal{Z}_{\tau,h}^{r,s+1}$  with  $\mathbf{u}_{\tau,h}^{k+1}(0) = \mathbf{0}$  such that

$$\begin{aligned} \sum_{n=1}^N \left\{ \int_{t_{n-1}}^{t_n} 2\mu \langle \boldsymbol{\varepsilon}(\mathbf{u}_{\tau,h}^{k+1}), \boldsymbol{\varepsilon}(\mathbf{z}_{\tau,h}) \rangle dt + \int_{t_{n-1}}^{t_n} \lambda \langle \nabla \cdot \mathbf{u}_{\tau,h}^{k+1}, \nabla \cdot \mathbf{z}_{\tau,h} \rangle dt \right\} \\ = \sum_{n=1}^N \int_{t_{n-1}}^{t_n} l_{\mathbf{u}}^{k+1}(\mathbf{z}_{\tau,h}) dt \end{aligned} \quad (3.9)$$

for all  $\mathbf{z}_{\tau,h} \in \widetilde{\mathcal{Z}}_{\tau,h}^{r-1,s+1}$ .

On the subinterval  $\bar{I}_n$  we expand the discrete functions  $p_{\tau,h}^k \in \mathcal{W}_{\tau,h}^{r,s}$ ,  $\mathbf{q}_{\tau,h}^k \in \mathcal{V}_{\tau,h}^{r,s}$  and  $\mathbf{u}_{\tau,h}^k \in \mathcal{H}_{\tau,h}^{r,s+1}$  in terms of Lagrangian basis functions  $\varphi_{n,j}$  with respect to  $r+1$  nodal points  $t_{n,j} \in \bar{I}_n$ ,  $j = 0, \dots, r$ , for the time variable such that they admit the representations

$$p_{\tau,h|I_n}^k(t) = \sum_{j=0}^r P_{n,h}^{j,k} \varphi_{n,j}(t), \quad \mathbf{q}_{\tau,h|I_n}^k(t) = \sum_{j=0}^r \mathbf{Q}_{n,h}^{j,k} \varphi_{n,j}(t), \quad \mathbf{u}_{\tau,h|I_n}^k(t) = \sum_{j=0}^r \mathbf{U}_{n,h}^{j,k} \varphi_{n,j}(t) \quad (3.10)$$

for  $t \in \bar{I}_n$  with coefficient functions  $P_{n,h}^{j,k} \in W_h$ ,  $\mathbf{Q}_{n,h}^{j,k} \in \mathbf{V}_h$  and  $\mathbf{U}_{n,h}^{j,k} \in \mathbf{H}_h$  for  $j = 0, \dots, r$ . Then we replace the variational problems (3.7), (3.8) and (3.9) by the following system of equations: Let  $n \in \{1, \dots, N\}$ . Find coefficient functions  $P_{n,h}^{i,k+1} \in W_h$  for  $i = 0, \dots, r$  and  $\mathbf{U}_{n,h}^{i,k+1} \in \mathbf{H}_h$ ,  $\mathbf{Q}_{n,h}^{i,k+1} \in \mathbf{V}_h$  for  $i = 1, \dots, r$  such that

$$\begin{aligned} \frac{1}{M} \sum_{j=0}^r \alpha_{ij} \langle P_{n,h}^{j,k+1}, w_h \rangle + L \sum_{j=0}^r \alpha_{ij} \langle P_{n,h}^{j,k+1} - P_{n,h}^{j,k}, w_h \rangle + \tau_n \beta_{ii} \langle \nabla \cdot \mathbf{Q}_{n,h}^{i,k+1}, w_h \rangle \\ = \tau_n \beta_{ii} \langle f(t_{n,i}), w_h \rangle - b \sum_{j=0}^r \alpha_{ij} \langle \nabla \cdot \mathbf{U}_{n,h}^{j,k}, w_h \rangle, \end{aligned} \quad (3.11)$$

$$\langle \mathbf{K}^{-1} \mathbf{Q}_{n,h}^{i,k+1}, \mathbf{v}_h \rangle - \langle P_{n,h}^{i,k+1}, \nabla \cdot \mathbf{v}_h \rangle = 0, \quad (3.12)$$

$$2\mu \langle \boldsymbol{\varepsilon}(\mathbf{U}_{n,h}^{i,k+1}), \boldsymbol{\varepsilon}(\mathbf{z}_h) \rangle + \lambda \langle \nabla \cdot \mathbf{U}_{n,h}^{i,k+1}, \nabla \cdot \mathbf{z}_h \rangle - b \langle P_{n,h}^{i,k+1}, \nabla \cdot \mathbf{z}_h \rangle = 0 \quad (3.13)$$

for all  $w_h \in W_h$ ,  $\mathbf{v}_h \in \mathbf{V}_h$ ,  $\mathbf{z}_h \in \mathbf{H}_h$  and  $i = 1, \dots, r$ , where  $P_{n,h}^{0,k+1}$  is defined by the continuity constraint in time of the discrete solution  $p_{\tau,h}^{k+1} \in \mathcal{W}_{\tau,h}^{r,s}$ , i.e.  $P_{n,h}^{0,k+1} = \lim_{l \rightarrow \infty} p_{\tau,h}^l|_{I_{n-1}}(t_{n-1})$  for  $n > 1$  and  $P_{n,h}^{0,k+1} = 0$  for  $n = 1$ .

The coefficients  $\alpha_{ij}$  and  $\beta_{ii}$  in (3.11)–(3.13) are defined by

$$\alpha_{ij} = \int_{I_n} \varphi'_{n,j}(t) \cdot \varphi_{n,i}(t) dt, \quad \beta_{ii} = \int_{I_n} \varphi_{n,i}(t) \cdot \varphi_{n,i}(t) dt, \quad i = 1, \dots, r, \quad j = 0, \dots, r.$$

**Remark 3.1** • The scheme (3.7)–(3.9) defines a Galerkin–Petrov method, since the trial spaces (3.1)–(3.3) and test spaces (3.4)–(3.6) differ.

- For all technical details of the derivation of the semi-algebraic equations (3.11)–(3.13) we refer to, e.g., [6, 7, 23, 37].
- We note that (3.11)–(3.13) is not the local counterpart of (3.7)–(3.9) on  $I_n$ , i.e. the formulation of (3.11)–(3.13) on the subinterval  $I_n$  by a suitable choice of a test basis in time with support in  $\bar{I}_n$  (cf. [6, 7, 23, 37]), since in (3.7)–(3.9) the iteration process is performed globally on  $\bar{I}$ . In contrast to this, the scheme (3.11)–(3.13) is based on iterating on each of the subintervals  $I_n$  before proceeding to the next one.
- For the treatment of the continuity constraint in time we put  $t_{n,0} = t_{n-1}$  for the nodal points of the Lagrangian basis functions. The other points  $t_{n,1}, \dots, t_{n,r}$  are chosen as the quadrature points of the  $r$ -point Gauss quadrature formula on  $I_n$  which is exact if the function to be integrated is a polynomial of degree less or equal to  $2r - 1$ . In particular, there holds that  $\varphi_{n,j}(t_{n,i}) = \delta_{i,j}$  for  $i, j = 0, \dots, r$ .
- The variational formulations (3.11)–(3.13) solely depend on the values of the flux and the displacement variable in the Gauss quadrature points as Eqs. (3.11) and (3.13) show, i.e. they depend on  $\mathbf{Q}_{n,h}^{i,k+1}$  and  $\mathbf{U}_{n,h}^{i,k+1}$  for  $i = 1, \dots, r$ . We then define the flux and the displacement variable in the grid points by extrapolation, in this way also ensuring the continuity in time, i.e.  $\mathbf{Q}_{n,h}^{0,k+1} = \mathbf{q}_{\tau,h}|_{I_{n-1}}(t_{n-1})$  and  $\mathbf{U}_{n,h}^{0,k+1} = \mathbf{u}_{\tau,h}|_{I_{n-1}}(t_{n-1})$ ; cf. [6, 7, 23, 37].
- We define the discrete initial flux as a suitable finite element approximation in  $\mathbf{V}_h$  of  $\mathbf{q}(0) = -\mathbf{K}\nabla p_0$ , if  $p_0$  is sufficiently regular. If this is not the case we take a regular approximation. The discrete initial flux is only needed for having a consistent notation and the extrapolation argument of the previous item in the first subinterval  $I_1$ . The discrete initial flux is of no relevance for the analysis of the scheme.

### 3.2 The dG( $r$ )–MFEM( $s$ )cG( $s+1$ ) approach.

The space-time finite element approximation of the flow problem (2.7), (2.8) by a discontinuous finite element approach in time (cf. [13, 41, 6, 22]) reads as follows: Let  $\mathbf{u}_{\tau,h}^k \in \widetilde{\mathcal{Z}}_{\tau,h}^{r,s+1}$ ,  $p_{\tau,h}^k \in \widetilde{\mathcal{W}}_{\tau,h}^{r,s}$  be given and

$$l_p^k(\mathbf{w}_{\tau,h}) = \left\langle f - b\nabla \cdot \partial_t \mathbf{u}_{\tau,h}^k + L\partial_t p_{\tau,h}^k, \mathbf{w}_{\tau,h} \right\rangle,$$

for  $\mathbf{w}_{\tau,h} \in \widetilde{\mathcal{W}}_{\tau,h}^{r,s}$ . Find  $p_{\tau,h}^{k+1} \in \widetilde{\mathcal{W}}_{\tau,h}^{r,s}$  and  $\mathbf{q}_{\tau,h}^{k+1} \in \widetilde{\mathcal{V}}_{\tau,h}^{r,s}$  with  $p_{\tau,h}^{k+1}(0) = 0$  such that

$$\begin{aligned} & \sum_{n=1}^N \left\{ \int_{t_{n-1}}^{t_n} \left( \frac{1}{M} + L \right) \langle \partial_t p_{\tau,h}^{k+1}, w_{\tau,h} \rangle dt + \int_{t_{n-1}}^{t_n} \langle \nabla \cdot \mathbf{q}_{\tau,h}^{k+1}, w_{\tau,h} \rangle dt \right\} \\ & + \left( \frac{1}{M} + L \right) \left\langle [p_{\tau,h}^{k+1}]_{n-1}, w_{\tau,h}(t_{n-1}^+) \right\rangle = \sum_{n=1}^N \int_{t_{n-1}}^{t_n} l_p^k(w_{\tau,h}) dt \end{aligned} \quad (3.14)$$

$$+ L \left\langle [p_{\tau,h}^k]_{n-1}, w_{\tau,h}(t_{n-1}^+) \right\rangle - \left\langle [\nabla \cdot \mathbf{u}_{\tau,h}^k]_{n-1}, w_{\tau,h}(t_{n-1}^+) \right\rangle,$$

$$\sum_{n=1}^N \left\{ \int_{t_{n-1}}^{t_n} \langle \mathbf{K}^{-1} \mathbf{q}_{\tau,h}^{k+1}, \mathbf{v}_{\tau,h} \rangle dt - \int_{t_{n-1}}^{t_n} \langle p_{\tau,h}^{k+1}, \nabla \cdot \mathbf{v}_{\tau,h} \rangle dt \right\} = 0 \quad (3.15)$$

for all  $w_{\tau,h} \in \widetilde{\mathcal{W}}_{\tau,h}^{r,s}$  and  $\mathbf{v}_{\tau,h} \in \widetilde{\mathcal{V}}_{\tau,h}^{r,s}$ .

Here we use the notation

$$p_{\tau,h}^k(t_n^-) = \lim_{t \rightarrow t_n^-} p_{\tau,h}^k(t), \quad p_{\tau,h}^k(t_n^+) = \lim_{t \rightarrow t_n^+} p_{\tau,h}^k(t), \quad [p_{\tau,h}^k]_n = p_{\tau,h}^k(t_n^+) - p_{\tau,h}^k(t_n^-),$$

and analogously for the displacement field  $\mathbf{u}_{\tau,h}^k$ .

The corresponding space-time finite element approximation of the problem (2.9) of mechanical deformation reads as follows: Let  $p_{\tau,h}^{k+1} \in \widetilde{\mathcal{W}}_{\tau,h}^{r,s}$  be given and

$$l_{\mathbf{u}}^{k+1}(\mathbf{z}_{\tau,h}) = b \langle p_{\tau,h}^{k+1}, \nabla \cdot \mathbf{z}_{\tau,h} \rangle$$

for  $\mathbf{z}_{\tau,h} \in \widetilde{\mathcal{Z}}_{\tau,h}^{r,s+1}$ . Find  $\mathbf{u}_{\tau,h}^{k+1} \in \widetilde{\mathcal{Z}}_{\tau,h}^{r,s+1}$  with  $\mathbf{u}_{\tau,h}^{k+1}(0) = \mathbf{0}$  such that

$$\begin{aligned} & \sum_{n=1}^N \left\{ \int_{t_{n-1}}^{t_n} 2\mu \langle \boldsymbol{\varepsilon}(\mathbf{u}_{\tau,h}^{k+1}), \boldsymbol{\varepsilon}(\mathbf{z}_{\tau,h}) \rangle dt + \int_{t_{n-1}}^{t_n} \lambda \langle \nabla \cdot \mathbf{u}_{\tau,h}^{k+1}, \nabla \cdot \mathbf{z}_{\tau,h} \rangle dt \right\} \\ & = \sum_{n=1}^N \int_{t_{n-1}}^{t_n} l_{\mathbf{u}}^{k+1}(\mathbf{z}_{\tau,h}) dt \end{aligned} \quad (3.16)$$

for all  $\mathbf{z}_{\tau,h} \in \widetilde{\mathcal{Z}}_{\tau,h}^{r,s+1}$ .

On  $I_n$  we expand the discrete functions  $p_{\tau,h}^k \in \widetilde{\mathcal{W}}_{\tau,h}^{r,s}$ ,  $\mathbf{q}_{\tau,h}^k \in \widetilde{\mathcal{V}}_{\tau,h}^{r,s}$  and  $\mathbf{u}_{\tau,h}^k \in \widetilde{\mathcal{Z}}_{\tau,h}^{r,s+1}$  in time in terms of Lagrangian basis functions  $\varphi_{n,j}$  with respect to  $r+1$  nodal points  $t_{n,j} \in I_n$ ,

$$p_{\tau,h|I_n}^k(t) = \sum_{j=0}^r P_{n,h}^{j,k} \varphi_{n,j}(t), \quad \mathbf{q}_{\tau,h|I_n}^k(t) = \sum_{j=0}^r \mathbf{Q}_{n,h}^{j,k} \varphi_{n,j}(t), \quad \mathbf{u}_{\tau,h|I_n}^k(t) = \sum_{j=0}^r \mathbf{U}_{n,h}^{j,k} \varphi_{n,j}(t) \quad (3.17)$$

for  $t \in I_n$  with coefficient functions  $P_{n,h}^{j,k} \in W_h$ ,  $\mathbf{Q}_{n,h}^{j,k} \in \mathbf{V}_h$  and  $\mathbf{U}_{n,h}^{j,k} \in \mathbf{H}_h$  for  $j = 0, \dots, r$ . The nodal points  $t_{n,j}$ , with  $j = 0, \dots, r$ , are chosen as the quadrature points of the  $r+1$ -point Gauss quadrature formula on  $I_n$  which is exact for polynomials of degree less or equal to  $2r+1$ .

Then we replace the variational problems (3.14), (3.15) and (3.16) by the following system of equations: Let  $n \in \{1, \dots, N\}$ . Find coefficient functions  $P_{n,h}^{i,k+1} \in W_h$ ,  $\mathbf{U}_{n,h}^{i,k+1} \in \mathbf{H}_h$  and

$\mathbf{Q}_{n,h}^{i,k+1} \in \mathbf{V}_h$  for  $i = 0, \dots, r$  such that

$$\begin{aligned} \frac{1}{M} \sum_{j=0}^r \tilde{\alpha}_{ij} \langle P_{n,h}^{j,k+1}, w_h \rangle + L \sum_{j=0}^r \tilde{\alpha}_{ij} \langle P_{n,h}^{j,k+1} - P_{n,h}^{j,k}, w_h \rangle + \tau_n \tilde{\beta}_{ii} \langle \nabla \cdot \mathbf{Q}_{n,h}^{i,k+1}, w_h \rangle \\ = \tau_n \tilde{\beta}_{ii} \langle f(t_{n,i}), w_h \rangle - b \sum_{j=0}^r \alpha_{ij} \langle \nabla \cdot \mathbf{U}_{n,h}^{j,k}, w_h \rangle \end{aligned} \quad (3.18)$$

$$\begin{aligned} + \gamma_i \frac{1}{M} \langle p_{\tau,h}^\infty(t_{n-1}^-), w_h \rangle + \gamma_i \langle b \nabla \cdot \mathbf{u}_{\tau,h}^\infty(t_{n-1}^-), w_h \rangle, \\ \langle \mathbf{K}^{-1} \mathbf{Q}_{n,h}^{i,k+1}, \mathbf{v}_h \rangle - \langle P_{n,h}^{i,k+1}, \nabla \cdot \mathbf{v}_h \rangle = 0, \end{aligned} \quad (3.19)$$

$$2\mu \langle \varepsilon(\mathbf{U}_{n,h}^{i,k+1}), \varepsilon(\mathbf{z}_h) \rangle + \lambda \langle \nabla \cdot \mathbf{U}_{n,h}^{i,k+1}, \nabla \cdot \mathbf{z}_h \rangle - b \langle P_{n,h}^{i,k+1}, \nabla \cdot \mathbf{z}_h \rangle = 0 \quad (3.20)$$

for all  $w_h \in W_h$ ,  $\mathbf{v}_h \in \mathbf{V}_h$ ,  $\mathbf{z}_h \in \mathbf{H}_h$  and  $i = 0, \dots, r$ , where  $p_{\tau,h}^\infty(t_{n-1}^-) = \lim_{l \rightarrow \infty} p_{\tau,h}^l(t_{n-1}^-)$  and  $\mathbf{u}_{\tau,h}^\infty(t_{n-1}^-) = \lim_{l \rightarrow \infty} \mathbf{u}_{\tau,h}^l(t_{n-1}^-)$  for  $n > 1$  as well as  $p_{\tau,h}(t_{n-1}^-) = 0$  and  $\mathbf{u}_{\tau,h}(t_{n-1}^-) = \mathbf{0}$  for  $n = 1$ .

The coefficients  $\tilde{\alpha}_{ij}$ ,  $\tilde{\beta}_{ii}$ ,  $\alpha_{ij}$  and  $\gamma_i$  are defined by

$$\tilde{\alpha}_{ij} = \alpha_{ij} + \gamma_i \cdot \gamma_j, \quad \tilde{\beta}_{ii} = \beta_{ii}, \quad \gamma_i = \varphi_{n,i}(t_{n-1}^+)$$

with

$$\alpha_{ij} = \int_{I_n} \varphi'_{n,j}(t) \cdot \varphi_{n,i}(t) dt, \quad \beta_{ii} = \int_{I_n} \varphi_{n,i}(t) \cdot \varphi_{n,i}(t) dt$$

for  $i, j = 0, \dots, r$ .

## 4 Convergence of the iteration schemes

Now we prove the convergence of the iterative splitting schemes that we introduced in Sec. 3.

### 4.1 The cGP( $r$ )–MFEM( $s$ )cG( $s+1$ ) approach.

In this subsection we prove the (linear) convergence of the splitting schemes (3.11)–(3.13) based on a continuous Galerkin discretization of the time variable. For this we show that the scheme is subject to a contraction principle such that a unique fixed point is obtained. This convergence is proved in strong energy norms.

In the sequel, we denote by  $p_{\tau,h} \in \mathcal{W}_{\tau,h}^{r,s}$ ,  $\mathbf{q}_{\tau,h} \in \mathcal{V}_{\tau,h}^{r,s}$  and  $\mathbf{u}_{\tau,h} \in \mathcal{Z}_{\tau,h}^{r,s+1}$ , with

$$p_{\tau,h|I_n}(t) = \sum_{j=0}^r P_{n,h}^j \varphi_{n,j}(t), \quad \mathbf{q}_{\tau,h|I_n}(t) = \sum_{j=0}^r \mathbf{Q}_{n,h}^j \varphi_{n,j}(t), \quad \mathbf{u}_{\tau,h|I_n}(t) = \sum_{j=0}^r \mathbf{U}_{n,h}^j \varphi_{n,j}(t) \quad (4.1)$$

for  $t \in \bar{I}_n$ , the space-time finite element approximation of the Biot system (2.1)–(2.4) that is defined by skipping the upper indices in the problems (3.7), (3.8) and (3.9), respectively. Thus we tacitly suppose that the coupled system that is obtained by discretizing the Biot model (2.1)–(2.4) in the space-time finite element spaces (3.1)–(3.3) admits a unique solution. By means of our variational framework for the time discretization the existence and uniqueness of the solution can be shown along the lines of [30, Part I, Sec. 4], where the proof is given for the spatially semidiscretized problem.

For the sake of brevity, we define the following variables quantifying the errors between this space-time finite element approximation of the Biot system (2.1)–(2.4) and its approximation after  $k$  iterations of the proposed scheme (3.11)–(3.13). For fixed  $n \in \{1, \dots, N\}$  we put

$$\begin{aligned} E_p^{j,k} &= P_{n,h}^{j,k} - P_{n,h}^j, \quad j \in \{0, \dots, r\}, & e_p^k(t) &= \sum_{j=0}^r E_p^{j,k} \varphi_{n,j}(t), \quad t \in \bar{I}_n, \\ \mathbf{E}_q^{j,k} &= \mathbf{Q}_{n,h}^{j,k} - \mathbf{Q}_{n,h}^j, \quad j \in \{0, \dots, r\}, & e_q^k(t) &= \sum_{j=0}^r \mathbf{E}_q^{j,k} \varphi_{n,j}(t), \quad t \in \bar{I}_n, \\ \mathbf{E}_u^{j,k} &= \mathbf{U}_{n,h}^{j,k} - \mathbf{U}_{n,h}^j, \quad j \in \{0, \dots, r\}, & e_u^k(t) &= \sum_{j=0}^r \mathbf{E}_u^{j,k} \varphi_{n,j}(t), \quad t \in \bar{I}_n. \end{aligned}$$

In order to simplify the notation below, we further introduce the abbreviations

$$S_p^{i,k+1} = \sum_{j=0}^r \alpha_{ij} E_p^{j,k+1}, \quad \mathbf{S}_q^{i,k+1} = \sum_{j=0}^r \alpha_{ij} \mathbf{E}_q^{j,k+1}, \quad \mathbf{S}_u^{i,k+1} = \sum_{j=0}^r \alpha_{ij} \mathbf{E}_u^{j,k+1} \quad (4.2)$$

with  $S_p^{i,k+1} \in W_h$ ,  $\mathbf{S}_q^{i,k+1} \in \mathbf{V}_h$  and  $\mathbf{S}_u^{i,k+1} \in \mathbf{H}_h$  for  $i = 1, \dots, r$ .

**Remark 4.1** *Due to the continuity constraint in time that is imposed by the definition of the space-time finite element spaces (3.1)–(3.3) and incorporated into the scheme (3.11)–(3.13) there holds that*

$$E_p^{0,k} = 0, \quad \mathbf{E}_q^{0,k} = \mathbf{0}, \quad \mathbf{E}_u^{0,k} = \mathbf{0} \quad (4.3)$$

for any iteration index  $k \in \mathbb{N}$ .

**Theorem 4.2** *Let  $p_{\tau,h} \in \mathcal{W}_{\tau,h}^{r,s}$ ,  $\mathbf{q}_{\tau,h} \in \mathbf{V}_{\tau,h}^{r,s}$  and  $\mathbf{u}_{\tau,h} \in \mathcal{Z}_{\tau,h}^{r,s+1}$  denote the fully discrete space-time finite element approximation of the Biot system (2.1)–(2.4). On  $I_n$  let  $\{p_{\tau,h}, \mathbf{q}_{\tau,h}, \mathbf{u}_{\tau,h}\}$  be represented by (4.1) and let  $\{p_{\tau,h}^k, \mathbf{q}_{\tau,h}^k, \mathbf{u}_{\tau,h}^k\}$  be defined by (3.10) with coefficient functions being given by the scheme (3.11)–(3.13). Then, for any  $L \geq b^2/(2\lambda)$  the sequence  $\{S_p^{i,k}\}_k$ , for  $i = 1, \dots, r$ , converges geometrically in  $W_h$ . For  $n = 1, \dots, N$  this implies the convergence of  $\{p_{\tau,h}^k(t_n), \mathbf{q}_{\tau,h}^k(t_n), \mathbf{u}_{\tau,h}^k(t_n)\}$  to  $\{p_{\tau,h}(t_n), \mathbf{q}_{\tau,h}(t_n), \mathbf{u}_{\tau,h}(t_n)\}$  in  $W_h \times \mathbf{V}_h \times \mathbf{H}_h$  for  $k \rightarrow \infty$ .*

**Proof.** We split the proof into several steps.

**1. Step (Error equations).** By subtracting equations (3.11)–(3.13) from the system that is obtained by discretizing the coupled Biot model (2.1)–(2.4) in the space-time finite element spaces (3.1)–(3.3), respectively, we obtain the error equations

$$\begin{aligned} \frac{1}{M} \sum_{j=0}^r \alpha_{ij} \langle E_p^{j,k+1}, w_h \rangle + L \sum_{j=0}^r \alpha_{ij} \langle E_p^{j,k+1} - E_p^{j,k}, w_h \rangle \\ + \tau_n \beta_{ii} \langle \nabla \cdot \mathbf{E}_q^{i,k+1}, w_h \rangle = -b \sum_{j=0}^r \alpha_{ij} \langle \nabla \cdot \mathbf{E}_u^{j,k}, w_h \rangle, \end{aligned} \quad (4.4)$$

$$\langle \mathbf{K}^{-1} \mathbf{E}_q^{i,k+1}, \mathbf{v}_h \rangle - \langle E_p^{i,k+1}, \nabla \cdot \mathbf{v}_h \rangle = 0, \quad (4.5)$$

$$2\mu \langle \boldsymbol{\varepsilon}(\mathbf{E}_u^{i,k+1}), \boldsymbol{\varepsilon}(\mathbf{z}_h) \rangle + \lambda \langle \nabla \cdot \mathbf{E}_u^{i,k+1}, \nabla \cdot \mathbf{z}_h \rangle - b \langle E_p^{i,k+1}, \nabla \cdot \mathbf{z}_h \rangle = 0 \quad (4.6)$$

for all  $w_h \in W_h$ ,  $\mathbf{v}_h \in \mathbf{V}_h$ ,  $\mathbf{z}_h \in \mathbf{H}_h$  and  $i = 1, \dots, r$ .

In the next steps we choose appropriate test functions in the Eqs. (4.4)–(4.6), respectively, and sum up resulting identities.

**2. Step (Choice of test function in Eq. (4.4)).** We test Eq. (4.4) with  $w_h = \sum_{j=0}^r \alpha_{ij} E_p^{j,k+1}$  to get that

$$\begin{aligned} \frac{1}{M} \left\| \sum_{j=0}^r \alpha_{ij} E_p^{j,k+1} \right\|^2 + L \left\langle \sum_{j=0}^r \alpha_{ij} (E_p^{j,k+1} - E_p^{j,k}), \sum_{j=0}^r \alpha_{ij} E_p^{j,k+1} \right\rangle \\ + \tau_n \beta_{ii} \left\langle \nabla \cdot \mathbf{E}_q^{i,k+1}, \sum_{j=0}^r \alpha_{ij} E_p^{j,k+1} \right\rangle = -b \left\langle \sum_{j=0}^r \alpha_{ij} \nabla \cdot \mathbf{E}_u^{j,k}, \sum_{j=0}^r \alpha_{ij} E_p^{j,k+1} \right\rangle \end{aligned} \quad (4.7)$$

for any  $i \in \{1, \dots, r\}$ . Using the notation (4.2), we can rewrite Eq. (4.7) as

$$\begin{aligned} \frac{1}{M} \|S_p^{i,k+1}\|^2 + L \langle S_p^{i,k+1} - S_p^{i,k}, S_p^{i,k+1} \rangle + \tau_n \beta_{ii} \langle \nabla \cdot \mathbf{E}_q^{i,k+1}, S_p^{i,k+1} \rangle \\ = -b \langle \nabla \cdot \mathbf{S}_u^{i,k}, S_p^{i,k+1} \rangle. \end{aligned} \quad (4.8)$$

We note that  $\beta_{ii} > 0$  for  $i = 0, \dots, r$ ; cf. [7, Lemma 2.2]. Now, dividing Eq. (4.8) by  $\beta_{ii}$  and using the algebraic identity

$$\langle x - y, x \rangle = \frac{1}{2} \|x\|^2 + \frac{1}{2} \|x - y\|^2 - \frac{1}{2} \|y\|^2$$

we recover Eq. (4.8) in the equivalent form that

$$\begin{aligned} \left( \frac{1}{M\beta_{ii}} + \frac{L}{2\beta_{ii}} \right) \|S_p^{i,k+1}\|^2 + \frac{L}{2\beta_{ii}} \|S_p^{i,k+1} - S_p^{i,k}\|^2 - \frac{L}{2\beta_{ii}} \|S_p^{i,k}\|^2 \\ + \tau_n \langle \nabla \cdot \mathbf{E}_q^{i,k+1}, S_p^{i,k+1} \rangle = -\frac{b}{\beta_{ii}} \langle \nabla \cdot \mathbf{S}_u^{i,k}, S_p^{i,k+1} \rangle \end{aligned} \quad (4.9)$$

for  $i = 1, \dots, r$ .

**3. Step (Summation of Eq. (4.5) and choice of test function).** Firstly, we note that Eq. (4.5) is also satisfied for  $i = 0$  by means of the observation (4.3). Changing the index  $i$  in Eq. (4.5) to  $j$ , multiplying the resulting equation with  $\alpha_{ij}$  and, then, summing up from  $j = 0$  to  $r$  and recalling Eq. (4.2) yields that

$$\langle \mathbf{K}^{-1} \mathbf{S}_q^{i,k+1}, \mathbf{v}_h \rangle - \langle S_p^{i,k+1}, \nabla \cdot \mathbf{v}_h \rangle = 0 \quad (4.10)$$

for all  $\mathbf{v}_h \in \mathbf{V}_h$  and  $i = 1, \dots, r$ . Testing Eq. (4.10) with  $\mathbf{v}_h = \tau_n \mathbf{E}_q^{i,k+1} \in \mathbf{V}_h$  we get that

$$\tau_n \langle \mathbf{K}^{-1} \mathbf{S}_q^{i,k+1}, \mathbf{E}_q^{i,k+1} \rangle - \tau_n \langle S_p^{i,k+1}, \nabla \cdot \mathbf{E}_q^{i,k+1} \rangle = 0. \quad (4.11)$$

Adding Eq. (4.11) to Eq. (4.9) then gives that

$$\begin{aligned} \left( \frac{1}{M\beta_{ii}} + \frac{L}{2\beta_{ii}} \right) \|S_p^{i,k+1}\|^2 + \frac{L}{2\beta_{ii}} \|S_p^{i,k+1} - S_p^{i,k}\|^2 - \frac{L}{2\beta_{ii}} \|S_p^{i,k}\|^2 \\ + \tau_n \langle \mathbf{K}^{-1} \mathbf{S}_q^{i,k+1}, \mathbf{E}_q^{i,k+1} \rangle = -\frac{b}{\beta_{ii}} \langle \nabla \cdot \mathbf{S}_u^{i,k}, S_p^{i,k+1} \rangle \end{aligned} \quad (4.12)$$

for all  $i = 1, \dots, r$ .

**4. Step (Summation of Eq. (4.6) and choice of test function).** Similarly, we note that Eq. (4.6) is also satisfied for  $i = 0$  by means of the observation (4.3). Changing the index  $i$  in Eq. (4.6) to  $j$ , multiplying the resulting equation with  $\alpha_{ij}$  and, then, summing up from  $j = 0$  to  $r$  and recalling Eq. (4.2) yields that

$$2\mu \langle \varepsilon(\mathbf{S}_u^{i,k+1}), \varepsilon(\mathbf{z}_h) \rangle + \lambda \langle \nabla \cdot \mathbf{S}_u^{i,k+1}, \nabla \cdot \mathbf{z}_h \rangle - b \langle S_p^{i,k+1}, \nabla \cdot \mathbf{z}_h \rangle = 0 \quad (4.13)$$

for all  $\mathbf{z}_h \in \mathbf{H}_h$  and  $i = 1, \dots, r$ . Testing Eq. (4.13) with  $\mathbf{z}_h = \frac{1}{\beta_{ii}} \mathbf{S}_u^{i,k} \in \mathbf{H}_h$  yields that

$$\frac{2\mu}{\beta_{ii}} \langle \varepsilon(\mathbf{S}_u^{i,k+1}), \varepsilon(\mathbf{S}_u^{i,k}) \rangle + \frac{\lambda}{\beta_{ii}} \langle \nabla \cdot \mathbf{S}_u^{i,k+1}, \nabla \cdot \mathbf{S}_u^{i,k} \rangle - \frac{b}{\beta_{ii}} \langle S_p^{i,k+1}, \nabla \cdot \mathbf{S}_u^{i,k} \rangle = 0 \quad (4.14)$$

for  $i = 1, \dots, r$ , where we again used that  $\beta_{ii} > 0$ ; cf. [7, Lemma 2.2]. Adding Eq. (4.14) to Eq. (4.12) leads to

$$\begin{aligned} & \left( \frac{1}{M\beta_{ii}} + \frac{L}{2\beta_{ii}} \right) \|S_p^{i,k+1}\|^2 + \frac{L}{2\beta_{ii}} \|S_p^{i,k+1} - S_p^{i,k}\|^2 + \tau_n \langle \mathbf{K}^{-1} \mathbf{S}_q^{i,k+1}, \mathbf{E}_q^{i,k+1} \rangle \\ & + \frac{2\mu}{\beta_{ii}} \langle \varepsilon(\mathbf{S}_u^{i,k+1}), \varepsilon(\mathbf{S}_u^{i,k}) \rangle + \frac{\lambda}{\beta_{ii}} \langle \nabla \cdot \mathbf{S}_u^{i,k+1}, \nabla \cdot \mathbf{S}_u^{i,k} \rangle = \frac{L}{2\beta_{ii}} \|S_p^{i,k}\|^2 \end{aligned} \quad (4.15)$$

for  $i = 1, \dots, r$ .

In the next step we consider the resulting incremental equation that is obtained by subtracting Eq. (4.13) written for two consecutive iteration indices from each other.

**5. Step (Formation of incremental equation for (4.13), choice of test function and summation).** We return to Eq. (4.13), write it for two consecutive iterations,  $k$  and  $k + 1$ , and subtract the resulting equations from each other to obtain that

$$2\mu \langle \varepsilon(\mathbf{S}_u^{i,k+1} - \mathbf{S}_u^{i,k}), \varepsilon(\mathbf{z}_h) \rangle + \lambda \langle \nabla \cdot (\mathbf{S}_u^{i,k+1} - \mathbf{S}_u^{i,k}), \nabla \cdot \mathbf{z}_h \rangle - b \langle S_p^{i,k+1} - S_p^{i,k}, \nabla \cdot \mathbf{z}_h \rangle = 0 \quad (4.16)$$

for all  $\mathbf{z}_h \in \mathbf{H}_h$  and  $i = 1, \dots, r$ . Choosing  $\mathbf{z}_h = \mathbf{S}_u^{i,k+1} - \mathbf{S}_u^{i,k} \in \mathbf{H}_h$  in Eq. (4.16), we find that

$$2\mu \|\varepsilon(\mathbf{S}_u^{i,k+1} - \mathbf{S}_u^{i,k})\|^2 + \lambda \|\nabla \cdot (\mathbf{S}_u^{i,k+1} - \mathbf{S}_u^{i,k})\|^2 = b \langle S_p^{i,k+1} - S_p^{i,k}, \nabla \cdot (\mathbf{S}_u^{i,k+1} - \mathbf{S}_u^{i,k}) \rangle \quad (4.17)$$

for  $i = 1, \dots, r$ . By dividing Eq. (4.17) by  $\beta_{ii} > 0$  and summing up the resulting identity from  $i = 1$  to  $r$  we obtain that

$$\begin{aligned} & \sum_{i=1}^r \frac{2\mu}{\beta_{ii}} \|\varepsilon(\mathbf{S}_u^{i,k+1} - \mathbf{S}_u^{i,k})\|^2 + \sum_{i=1}^r \frac{\lambda}{\beta_{ii}} \|\nabla \cdot (\mathbf{S}_u^{i,k+1} - \mathbf{S}_u^{i,k})\|^2 \\ & = \sum_{i=1}^r \frac{b}{\beta_{ii}} \langle S_p^{i,k+1} - S_p^{i,k}, \nabla \cdot (\mathbf{S}_u^{i,k+1} - \mathbf{S}_u^{i,k}) \rangle. \end{aligned} \quad (4.18)$$

Further, from Eq. (4.17) we get by means of the inequality of Cauchy-Schwarz that

$$\lambda \|\nabla \cdot (\mathbf{S}_u^{i,k+1} - \mathbf{S}_u^{i,k})\| \leq b \|S_p^{i,k+1} - S_p^{i,k}\| \quad (4.19)$$



for  $i = 1, \dots, r$ .

Next, we combine the derived relations.

**6. Step (Summation of Eq. (4.15) over  $i$  and combination with derived relations).**

Using the algebraic identity

$$\langle x, y \rangle = \frac{1}{4} \|x + y\|^2 - \frac{1}{4} \|x - y\|^2,$$

we get from Eq. (4.15) that

$$\begin{aligned} & \left( \frac{1}{M\beta_{ii}} + \frac{L}{2\beta_{ii}} \right) \|S_p^{i,k+1}\|^2 + \frac{L}{2\beta_{ii}} \|S_p^{i,k+1} - S_p^{i,k}\|^2 + \tau_n \langle \mathbf{K}^{-1} \mathbf{S}_q^{i,k+1}, \mathbf{E}_q^{i,k+1} \rangle \\ & + \frac{\mu}{2\beta_{ii}} \|\varepsilon(\mathbf{S}_u^{i,k+1} + \mathbf{S}_u^{i,k})\|^2 + \frac{\lambda}{4\beta_{ii}} \|\nabla \cdot (\mathbf{S}_u^{i,k+1} + \mathbf{S}_u^{i,k})\|^2 \\ & - \frac{\mu}{2\beta_{ii}} \|\varepsilon(\mathbf{S}_u^{i,k+1} - \mathbf{S}_u^{i,k})\|^2 - \frac{\lambda}{4\beta_{ii}} \|\nabla \cdot (\mathbf{S}_u^{i,k+1} - \mathbf{S}_u^{i,k})\|^2 = \frac{L}{2\beta_{ii}} \|S_p^{i,k}\|^2 \end{aligned} \quad (4.20)$$

for  $i = 1, \dots, r$ . Summing up Eq. (4.20) from  $i = 1$  to  $r$  and using the relations (4.18) and (4.19), we find that

$$\begin{aligned} & \sum_{i=1}^r \left\{ \left( \frac{1}{M\beta_{ii}} + \frac{L}{2\beta_{ii}} \right) \|S_p^{i,k+1}\|^2 \right. \\ & \quad \left. + \frac{L}{2\beta_{ii}} \|S_p^{i,k+1} - S_p^{i,k}\|^2 + \tau_n \langle \mathbf{K}^{-1} \mathbf{S}_q^{i,k+1}, \mathbf{E}_q^{i,k+1} \rangle \right\} \\ & + \sum_{i=1}^r \left\{ \frac{\mu}{2\beta_{ii}} \|\varepsilon(\mathbf{S}_u^{i,k+1} + \mathbf{S}_u^{i,k})\|^2 + \frac{\lambda}{4\beta_{ii}} \|\nabla \cdot (\mathbf{S}_u^{i,k+1} + \mathbf{S}_u^{i,k})\|^2 \right\} \\ & \leq \sum_{i=1}^r \frac{L}{2\beta_{ii}} \|S_p^{i,k}\|^2 + \sum_{i=1}^r \frac{b}{4\beta_{ii}} \langle S_p^{i,k+1} - S_p^{i,k}, \nabla \cdot (\mathbf{S}_u^{i,k+1} - \mathbf{S}_u^{i,k}) \rangle \\ & \leq \sum_{i=1}^r \frac{L}{2\beta_{ii}} \|S_p^{i,k}\|^2 + \sum_{i=1}^r \frac{b^2}{4\lambda\beta_{ii}} \|S_p^{i,k+1} - S_p^{i,k}\|^2. \end{aligned} \quad (4.21)$$

From [7, Lemma 2.3] we conclude that

$$\begin{aligned} & \sum_{i=1}^r \langle \mathbf{K}^{-1} \mathbf{S}_q^{i,k+1}, \mathbf{E}_q^{i,k+1} \rangle \\ & = \frac{1}{2} \langle \mathbf{K}^{-1} \mathbf{e}_q^{k+1}(t_n), \mathbf{e}_q^{k+1}(t_n) \rangle - \frac{1}{2} \langle \mathbf{K}^{-1} \mathbf{e}_q^{k+1}(t_{n-1}), \mathbf{e}_q^{k+1}(t_{n-1}) \rangle \\ & = \frac{1}{2} \langle \mathbf{K}^{-1} \mathbf{e}_q^{k+1}(t_n), \mathbf{e}_q^{k+1}(t_n) \rangle \geq \frac{k}{2} \|\mathbf{e}_q^{k+1}(t_n)\|^2, \end{aligned} \quad (4.22)$$

due to  $\mathbf{e}_q^{k+1}(t_{n-1}) = \mathbf{0}$  by means of Eq. (4.3). In Eq. (4.22) the constant  $k$  denotes the lower bound of the uniformly positive definite matrix  $\mathbf{K}^{-1}$ .

We are now in a position to perform our final contraction argument.

**7. Step (Contraction argument).** Combining Eq. (4.21) with Eq. (4.22) shows that

$$\begin{aligned} \sum_{i=1}^r \left( \frac{1}{M\beta_{ii}} + \frac{L}{2\beta_{ii}} \right) \|S_p^{i,k+1}\|^2 + \sum_{i=1}^r \frac{L}{2\beta_{ii}} \|S_p^{i,k+1} - S_p^{i,k}\|^2 + k \frac{\tau_n}{2} \|\mathbf{e}_q^{k+1}(t_n)\|^2 \\ \leq \sum_{i=1}^r \frac{L}{2\beta_{ii}} \|S_p^{i,k}\|^2 + \sum_{i=1}^r \frac{b^2}{4\lambda\beta_{ii}} \|S_p^{i,k+1} - S_p^{i,k}\|^2. \end{aligned} \quad (4.23)$$

The inequality (4.23) shows the geometric convergence of the iterates  $S_p^{i,k}$  in  $W_h$ , for  $i = 1, \dots, r$ , for any parameter  $L \geq b^2/(2\lambda)$ . The optimal choice of  $L$ , still ensuring the geometric convergence, is thus given by  $L = b^2/(2\lambda)$ . The geometric convergence of  $S_p^{i,k}$  along with Eq. (4.23) then implies the convergence of  $\mathbf{e}_q^k(t_n)$  to  $\mathbf{0}$  for  $k \rightarrow \infty$ .

By using error equation (4.5) for Darcy's law together with the convergence of  $\mathbf{e}_q^k(t_n)$  to  $\mathbf{0}$  for  $k \rightarrow \infty$  we directly get the convergence of  $e_p^k(t_n)$  to 0 for  $k \rightarrow \infty$ . Moreover, the error equation (4.6) for the subproblem of mechanics deformation along with the previous convergence results then implies the convergence of  $\mathbf{e}_u^k(t_n)$  to  $\mathbf{0}$  for  $k \rightarrow \infty$ . This proves the assertion of the theorem.  $\blacksquare$

**Remark 4.3** *The optimal constant  $L = b^2/(2\lambda)$  identified in the previous proof is the same as the one that is obtained in Thm. 2.1 for the iteration scheme (2.7), (2.8) and (2.9) on the level of the partial differential equations, even though different different techniques of proof are applied in Thm. 2.1 and Thm. 4.2, respectively. We note that the optimal choice of  $L$  does not depend on the time stepping scheme, i.e. on the particular choice of the parameter  $r$ . Moreover, our result is consistent to the analysis given in [27] where a convergence proof is given for the continuous case of subproblems of partial differential equations with the flow problem being written in a non-mixed setting.*

**Corollary 4.4** *For  $j = 0, \dots, r$ , the iterates  $\{P_{n,h}^{j,k}, \mathbf{Q}_{n,h}^{j,k}, \mathbf{U}_{n,h}^{j,k}\}$  converge to  $\{P_{n,h}^j, \mathbf{Q}_{n,h}^j, \mathbf{U}_{n,h}^j\}$  for  $k \rightarrow \infty$  in  $W_h \times \mathbf{V}_h \times \mathbf{H}_h$ . This implies the convergence of  $p_{\tau,h}^k$ ,  $\mathbf{q}_{\tau,h}^k$  and  $\mathbf{u}_{\tau,h}^k$  in  $L^2(I_n; W)$  and  $L^2(I_n; \mathbf{L}^2(\Omega))$ , respectively.*

**Proof.** From [7, Lemma 2.3] along with the first of the identities (4.3) we conclude that

$$\frac{1}{2} \|E_p^k(t_n)\|^2 = \int_{t_{n-1}}^{t_n} \langle \partial_t e_p^k, e_p^k \rangle dt = \sum_{i=1}^r \sum_{j=1}^r \alpha_{ij} \langle E_p^{j,k}, E_p^{i,k} \rangle. \quad (4.24)$$

Since the matrix  $(\alpha_{ij})_{i,j=1,\dots,r}$  in Eq. (4.24) is positive definite (cf. [20, p. 1784]) it follows that

$$\frac{1}{2} \|E_p^k(t_n)\|^2 \geq \alpha_0 \sum_{j=1}^r \|E_p^{j,k}\|^2 \quad (4.25)$$

with some constant  $\alpha_0 > 0$ . From (4.25) along with Thm. 4.2 we conclude the convergence of  $P_{n,h}^{j,k}$  in  $W_h$ . The convergence of  $E_q^{i,k}$  and  $E_u^{i,k}$  to  $\mathbf{0}$  for  $k \rightarrow \infty$  is then a direct consequence of (4.5) and (4.6), respectively. Finally, the convergence of  $p_{\tau,h}^k$  in  $L^2(I_n; W)$  and of  $\mathbf{q}_{\tau,h}^k$ ,  $\mathbf{u}_{\tau,h}^k$  in  $L^2(I_n; \mathbf{L}^2(\Omega))$  follows from the second result in [7, Lemma 2.3].  $\blacksquare$

## 4.2 The dG( $r$ )–MFEM( $s$ )cG( $s+1$ ) approach.

In this subsection we prove the (linear) convergence of the splitting schemes (3.18)–(3.20) based on a discontinuous Galerkin discretization of the time variable. Again, we show that the scheme is subject to a contraction principle such that a unique a fixed point is obtained.

In the sequel, we denote by  $p_{\tau,h} \in \widetilde{\mathcal{W}}_{\tau,h}^{r,s}$ ,  $\mathbf{q}_{\tau,h} \in \widetilde{\mathcal{V}}_{\tau,h}^{r,s}$  and  $\mathbf{u}_{\tau,h} \in \widetilde{\mathcal{Z}}_{\tau,h}^{r,s+1}$ , with

$$p_{\tau,h|I_n}(t) = \sum_{j=0}^r P_{n,h}^j \varphi_{n,j}(t), \quad \mathbf{q}_{\tau,h|I_n}(t) = \sum_{j=0}^r \mathbf{Q}_{n,h}^j \varphi_{n,j}(t), \quad \mathbf{u}_{\tau,h|I_n}(t) = \sum_{j=0}^r \mathbf{U}_{n,h}^j \varphi_{n,j}(t) \quad (4.26)$$

for  $t \in I_n$ , the space-time finite element approximation of the Biot system (2.1)–(2.4) that is defined by skipping the upper indices in the problems (3.14), (3.15) and (3.16), respectively. Thus we tacitly suppose that the coupled system that is obtained by discretizing the Biot model (2.1)–(2.4) in the space-time finite element spaces (3.4)–(3.6) admits a unique solution.

**Theorem 4.5** *Let  $p_{\tau,h} \in \widetilde{\mathcal{W}}_{\tau,h}^{r,s}$ ,  $\mathbf{q}_{\tau,h} \in \widetilde{\mathcal{V}}_{\tau,h}^{r,s}$  and  $\mathbf{u}_{\tau,h} \in \widetilde{\mathcal{Z}}_{\tau,h}^{r,s+1}$  denote the fully discrete space-time finite element approximation of the Biot system (2.1)–(2.4). On  $I_n$  let  $\{p_{\tau,h}, \mathbf{q}_{\tau,h}, \mathbf{u}_{\tau,h}\}$  be represented by (4.26) and let  $\{p_{\tau,h}^k, \mathbf{q}_{\tau,h}^k, \mathbf{u}_{\tau,h}^k\}$  be defined by (3.17) with coefficient functions being given by the scheme (3.18)–(3.20). Then, for any  $L \geq b^2/(2\lambda)$  the sequence  $\{S_p^{i,k}\}_k$ , for  $i = 1, \dots, r$ , converges geometrically in  $W_h$ . For  $n = 1, \dots, N$  this implies the convergence of  $\{p_{\tau,h}^k(t_n^\pm), \mathbf{q}_{\tau,h}^k(t_n^\pm), \mathbf{u}_{\tau,h}^k(t_n^\pm)\}$  to  $\{p_{\tau,h}(t_n^\pm), \mathbf{q}_{\tau,h}(t_n^\pm), \mathbf{u}_{\tau,h}(t_n^\pm)\}$  in  $W_h \times \mathbf{V}_h \times \mathbf{H}_h$  for  $k \rightarrow \infty$ .*

**Proof.** The proof follows the lines of the proof of Thm. 4.2. Therefore, we restrict ourselves to presenting the differences only. We use the notation and abbreviations of Subsec. 4.1.

We put

$$S_p^{i,k+1} = \sum_{j=0}^r \tilde{\alpha}_{ij} E_p^{j,k+1}, \quad S_q^{i,k+1} = \sum_{j=0}^r \tilde{\alpha}_{ij} \mathbf{E}_q^{j,k+1}, \quad S_u^{i,k+1} = \sum_{j=0}^r \tilde{\alpha}_{ij} \mathbf{E}_u^{j,k+1}$$

with  $S_p^{i,k+1} \in W_h$ ,  $S_q^{i,k+1} \in \mathbf{V}_h$  and  $S_u^{i,k+1} \in \mathbf{H}_h$  for  $i = 0, \dots, r$ . By the same arguments as in the proof of Thm. 4.2 we find that

$$\begin{aligned} & \sum_{i=0}^r \left\{ \left( \frac{1}{M\beta_{ii}} + \frac{L}{2\beta_{ii}} \right) \|S_p^{i,k+1}\|^2 + \frac{L}{2\beta_{ii}} \|S_p^{i,k+1} - S_p^{i,k}\|^2 + \tau_n \langle \mathbf{K}^{-1} S_q^{i,k+1}, \mathbf{E}_q^{i,k+1} \rangle \right\} \\ & + \sum_{i=0}^r \left\{ \frac{\mu}{2\beta_{ii}} \|\varepsilon(S_u^{i,k+1} + S_u^{i,k})\|^2 + \frac{\lambda}{4\beta_{ii}} \|\nabla \cdot (S_u^{i,k+1} + S_u^{i,k})\|^2 \right\} \\ & \leq \sum_{i=0}^r \frac{L}{2\beta_{ii}} \|S_p^{i,k}\|^2 + \sum_{i=0}^r \frac{b^2}{4\lambda\beta_{ii}} \|S_p^{i,k+1} - S_p^{i,k}\|^2. \end{aligned} \quad (4.27)$$

From [7, Lemma 2.3] we get that

$$\begin{aligned}
& \sum_{i=0}^r \langle \mathbf{K}^{-1} \mathbf{S}_q^{i,k+1}, \mathbf{E}_q^{i,k+1} \rangle \\
&= \sum_{i=0}^r \left\langle \mathbf{K}^{-1} \sum_{j=0}^r \alpha_{ij} \mathbf{E}_q^{j,k+1}, \mathbf{E}_q^{i,k+1} \right\rangle + \sum_{i=0}^r \left\langle \mathbf{K}^{-1} \sum_{j=0}^r \gamma_i \gamma_j \mathbf{E}_q^{j,k+1}, \mathbf{E}_q^{i,k+1} \right\rangle \\
&= \frac{1}{2} \langle \mathbf{K}^{-1} \mathbf{E}_q^{k+1}(t_n^-), \mathbf{e}_q^{k+1}(t_n^-) \rangle - \frac{1}{2} \langle \mathbf{K}^{-1} \mathbf{e}_q^{k+1}(t_{n-1}^+), \mathbf{e}_q^{k+1}(t_{n-1}^+) \rangle \\
&\quad + \left\langle \mathbf{K}^{-1} \sum_{j=0}^r \gamma_j \mathbf{E}_q^{j,k+1}, \sum_{i=0}^r \gamma_i \mathbf{E}_q^{i,k+1} \right\rangle \\
&= \frac{1}{2} \langle \mathbf{K}^{-1} \mathbf{e}_q^{k+1}(t_n^-), \mathbf{e}_q^{k+1}(t_n^-) \rangle + \frac{1}{2} \langle \mathbf{K}^{-1} \mathbf{e}_q^{k+1}(t_{n-1}^+), \mathbf{e}_q^{k+1}(t_{n-1}^+) \rangle, \tag{4.28}
\end{aligned}$$

where we used that

$$\left\langle \mathbf{K}^{-1} \sum_{j=0}^r \gamma_j \mathbf{E}_q^{j,k+1}, \sum_{i=0}^r \gamma_i \mathbf{E}_q^{i,k+1} \right\rangle = \langle \mathbf{K}^{-1} \mathbf{e}_q^{k+1}(t_{n-1}^+), \mathbf{e}_q^{k+1}(t_{n-1}^+) \rangle.$$

We are now in a position to perform our final contraction argument. Combining Eq. (4.27) with Eq. (4.28) shows that

$$\begin{aligned}
& \sum_{i=0}^r \left( \frac{1}{M\beta_{ii}} + \frac{L}{2\beta_{ii}} \right) \|S_p^{i,k+1}\|^2 + \sum_{i=0}^r \frac{L}{2\beta_{ii}} \|S_p^{i,k+1} - S_p^{i,k}\|^2 \\
&\quad + k \frac{\tau_n}{2} \|\mathbf{e}_q^{k+1}(t_n^-)\|^2 + k \frac{\tau_n}{2} \|\mathbf{e}_q^{k+1}(t_{n-1}^+)\|^2 \tag{4.29} \\
&\leq \sum_{i=0}^r \frac{L}{2\beta_{ii}} \|S_p^{i,k}\|^2 + \sum_{i=0}^r \frac{b^2}{4\lambda\beta_{ii}} \|S_p^{i,k+1} - S_p^{i,k}\|^2.
\end{aligned}$$

The inequality (4.29) shows the geometric convergence of the iterates  $S_p^{i,k}$  in  $W_h$ , for  $i = 0, \dots, r$ , for any parameter  $L \geq b^2/(2\lambda)$ . Again, the optimal choice of  $L$  is given by  $L = b^2/(2\lambda)$ . The geometric convergence of  $S_p^{i,k}$  along with Eq. (4.29) then implies the convergence of  $\mathbf{e}_q^k(t_{n-1}^+)$  and  $\mathbf{e}_q^k(t_n^-)$  to  $\mathbf{0}$  for  $k \rightarrow \infty$ .

By using error equation (4.5) for Darcy's law together with the convergence of  $\mathbf{e}_q^k(t_n^-)$  to  $\mathbf{0}$  for  $k \rightarrow \infty$  we directly get the convergence of  $e_p^k(t_n^-)$  to 0 for  $k \rightarrow \infty$ . Moreover, the error equation (4.6) for the subproblem of mechanics deformation along with the previous convergence results then implies the convergence of  $\mathbf{e}_u^k(t_n^-)$  to  $\mathbf{0}$  for  $k \rightarrow \infty$ . The convergence of  $e_p^k(t_{n-1}^+)$  to 0 and  $\mathbf{e}_u^k(t_{n-1}^+)$  to  $\mathbf{0}$  for  $k \rightarrow \infty$  follow similarly. ■

**Corollary 4.6** *For  $j = 0, \dots, r$ , the iterates  $\{P_{n,h}^{j,k}, \mathbf{Q}_{n,h}^{j,k}, \mathbf{U}_{n,h}^{j,k}\}$  converge to  $\{P_{n,h}^j, \mathbf{Q}_{n,h}^j, \mathbf{U}_{n,h}^j\}$  for  $k \rightarrow \infty$  in  $W_h \times \mathbf{V}_h \times \mathbf{H}_h$ . This implies the convergence of  $p_{\tau,h}^k, \mathbf{q}_{\tau,h}^k$  and  $\mathbf{u}_{\tau,h}^k$  in  $L^2(I_n; W)$  and  $L^2(I_n; \mathbf{L}^2(\Omega))$ , respectively.*

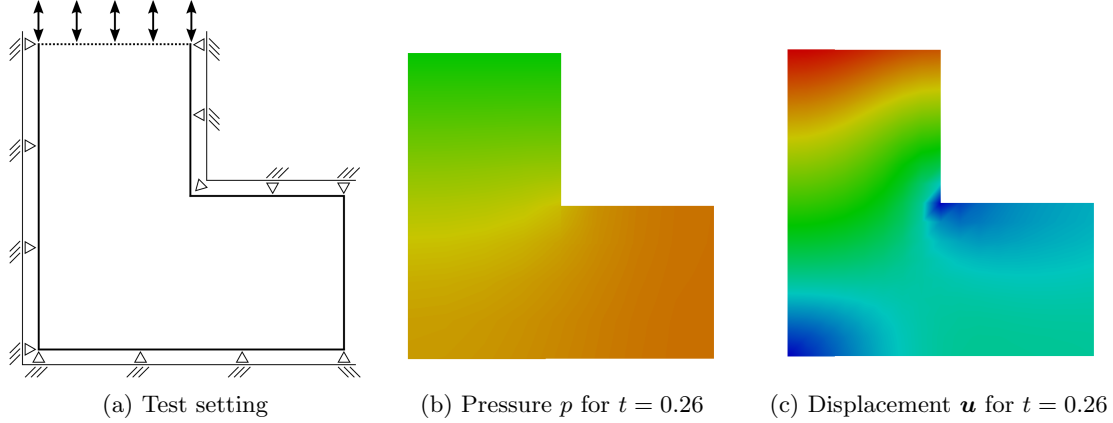


Figure 5.1: Test setting, pressure and magnitude of displacement field at  $t = 0.26$  for time step size  $\tau_n = 0.02$  and solver cGP(2)–MFEM(1)cG(2); cf. Sec. 3.1.

**Proof.** From [7, Lemma 2.3] we conclude that

$$\frac{1}{2} \|e_p^k(t_n^-)\|^2 - \frac{1}{2} \|e_p^k(t_{n-1}^+)\|^2 = \int_{t_{n-1}}^{t_n} \langle \partial_t e_p^k, e_p^k \rangle dt = \sum_{i=0}^r \sum_{j=0}^r \alpha_{ij} \langle E_p^{j,k}, E_p^{i,k} \rangle. \quad (4.30)$$

Since the matrix  $(\alpha_{ij})_{i,j=0,\dots,r}$  in Eq. (4.30) is positive definite (cf. [20, p. 1784]) it follows that

$$\frac{1}{2} \|e_p^k(t_n^-)\|^2 - \frac{1}{2} \|e_p^k(t_{n-1}^+)\|^2 \geq \alpha_0 \sum_{j=0}^r \|E_p^{j,k}\|^2$$

with some constant  $\alpha_0 > 0$ . Thm. 4.5 then implies the convergence of  $P^{j,k}$  to  $P^j$  for  $k \rightarrow \infty$  and  $j = 0, \dots, r$ . The convergence of  $\{\mathbf{Q}_{n,h}^{j,k}, \mathbf{U}_{n,h}^{j,k}\}$  to  $\{\mathbf{Q}_{n,h}^j, \mathbf{U}_{n,h}^j\}$  is now a direct consequence of (3.19) and (3.20), respectively. Finally, the convergence of  $e_p^k$ ,  $e_q^k$  and  $e_u^k$  to zero in  $L^2(I_n; W)$  and  $L^2(I_n; \mathbf{L}^2(\Omega))$ , respectively, follows from the exactness of the  $r+1$ -point Gauss quadrature formula on  $I_n$  all for polynomials of maximum degree  $2r + 1$ . ■

## 5 Numerical experiments

In this section we study the numerical performance properties of the fixed-stress iteration schemes (3.7)–(3.9) and (3.14)–(3.15), respectively, along with with the proposed choice of our analyses  $L = b/(2\lambda)$  for the numerical parameter  $L$ . For the time discretization we consider a continuous approximation with piecewise linear and quadratic polynomials, i.e. a cGP(1) and cGP(2) approach (cf. Sec. 3.1), as well as a discontinuous approximation with piecewise constant and linear polynomials, i.e. a dG(0) and dG(1) approach (cf. Sec. 3.2). In our computations we shall study numerically the sharpness of our theoretical result of Sec. 4 that  $L = b^2/(2\lambda)$  provides an optimal choice of  $L$  with respect to an acceleration of the convergence behaviour of the fixed point iterations. The implementation of the schemes is done in our front-end simulation tool for the latest deal.II version 8 library and allows distributed-parallel numerical simulations; cf. [5, 12, 23, 6] for details.

The problem setting of our test configuration with an L-shaped domain is sketched in Fig. 5.1. We consider solving the Biot problem in the time interval  $I = (0, 0.5)$ . We prescribed homogeneous initial conditions. The solid lines describe an undrained flow boundary (i.e.  $\mathbf{q} \cdot \mathbf{n} = 0$  with outer unit normal vector  $\mathbf{n}$ ) and the dashed line on the top describes a open flow boundary with a prescribed pressure value  $p = 0$ . At the open flow boundary at the top we prescribe a time-dependent traction boundary condition for mechanical deformation given by  $\boldsymbol{\sigma} \mathbf{n} = (0, h(t))^\top$ , with  $h(t) = -2560 t^2 (t - 0.5)^2$ . At the lower right boundary a homogeneous traction boundary condition is imposed. At all remaining boundaries we prescribe one displacement component to fulfil a homogeneous Dirichlet condition and the remaining component to fulfil a homogeneous traction boundary condition. The physical parameters are chosen as  $M = 100$ ,  $b = 100$ ,  $\mu = E/(2 \cdot (1 + \nu))$  and  $\lambda = E\nu/((1 - 2\nu) \cdot (1 + \nu))$  with  $E = 100$  and  $\nu = 0.35$  such that  $\mu = 37.037$  and  $\lambda = 86.42$ . Further we put  $\mathbf{K} = 0.1 \cdot \mathbf{I}$  with the identity matrix  $\mathbf{I}$ . Gravity is not considered, i.e.  $\mathbf{g} \equiv \mathbf{0}$ . The calculated profiles for fluid pressure and magnitude of displacement are illustrated exemplarily for  $t = 0.26$  in Fig. 5.1. For the pressure distribution the green coloured region corresponds to  $p(\cdot, 0.26) = 0$  and rises up to  $p(\cdot, 0.26) \approx 0.5$  in the orange coloured regions. For the displacement field magnitude distribution the blue coloured region corresponds to  $\|\mathbf{u}(\cdot, 0.26)\|_2 = 0$  and rises up to  $\|\mathbf{u}(\cdot, 0.26)\|_2 \approx 0.06$  in the red coloured region at the top of the domain.

As a stopping criterion for the fixed-stress iteration we prescribed a tolerance of  $\text{tol}_{\text{fixed}} = 1\text{e}-8$ , measured in the  $l^2$  norm, between two successive solution vectors for each of the unknown variables, i.e. pressure, flux and displacement field. For the lower order time discretizations dG(0) and cG(1) we chose  $\text{tol}_{\text{flow}} = 1\text{e}-14$  and  $\text{tol}_{\text{mechanics}} = 1\text{e}-12$  for the iterative solvers of the subproblems. For the higher order time discretisations dG(1) and cG(2) we put  $\text{tol}_{\text{flow}} = 1\text{e}-12$ , and  $\text{tol}_{\text{mechanics}} = 1\text{e}-12$  for the iterative solver tolerances.

In our first numerical study the sensitivity (cf. Fig. 5.2) of the iteration process with respect to choice of the spatial discretization step size  $h$  is analyzed. This is done for a lowest order in time discontinuous Galerkin discretization dG(0) and a MFEM(0)cG(1) approximation in space; cf. Sec. 3.2. In Fig. 5.2 the total number of iterations for all time steps in the interval  $I$  and step size  $\tau_n = 0.01$  is illustrated versus a perturbation  $\omega$  of our optimal choice of the numerical tuning parameter. Precisely, we performed our iterations with  $L = \omega \widehat{L}$  where  $\widehat{L} = b^2/(2\lambda)$  is the choice that is proposed by our analysis such that  $\omega = 1$  represents the theoretically expected result for the best performance of the iteration scheme with a minimum number of iterations. In Fig. 5.2 we observe a convergence behaviour that is almost independent of the refinement level  $m$  with  $h = 2^{-(m+1)}$ . For all refinement levels the computations show the optimal convergence behaviour for values slightly greater than one for the perturbation parameter,  $\omega \approx 1.05$ , such that our proposed choice of Sec. 4 corresponding to  $\omega = 1$  fits quite well. We note that for stronger perturbations of  $\omega = 1$  the number of required iterations increases strongly which leads to additional numerical costs.

In our second numerical study the sensitivity (cf. Fig. 5.3) of the iteration process with respect to a variation of the polynomial degree  $s$  of the spatial discretization is analyzed; cf. Sec. 3.1. We vary the parameter  $s$  from  $s = 1$  to  $s = 4$ . For the time discretization the lowest order continuous Galerkin approach cGP(1) is applied; cf. Sec. 3.1. In Fig. 5.3 we illustrate the total number of iterations for all time steps in the time interval  $I$  versus a perturbation of our proposed choice of the tuning parameter. As before,  $\omega = 1$  corresponds to the proposed value of our analysis in Sec. 4. Again, in our computations the iterations show strong robustness with respect to the choice of  $s$ . Therefore, the result of our analysis, corresponding to  $\omega = 1$ , is close to the optimal point of a minimum number of iterations. For the higher order variants

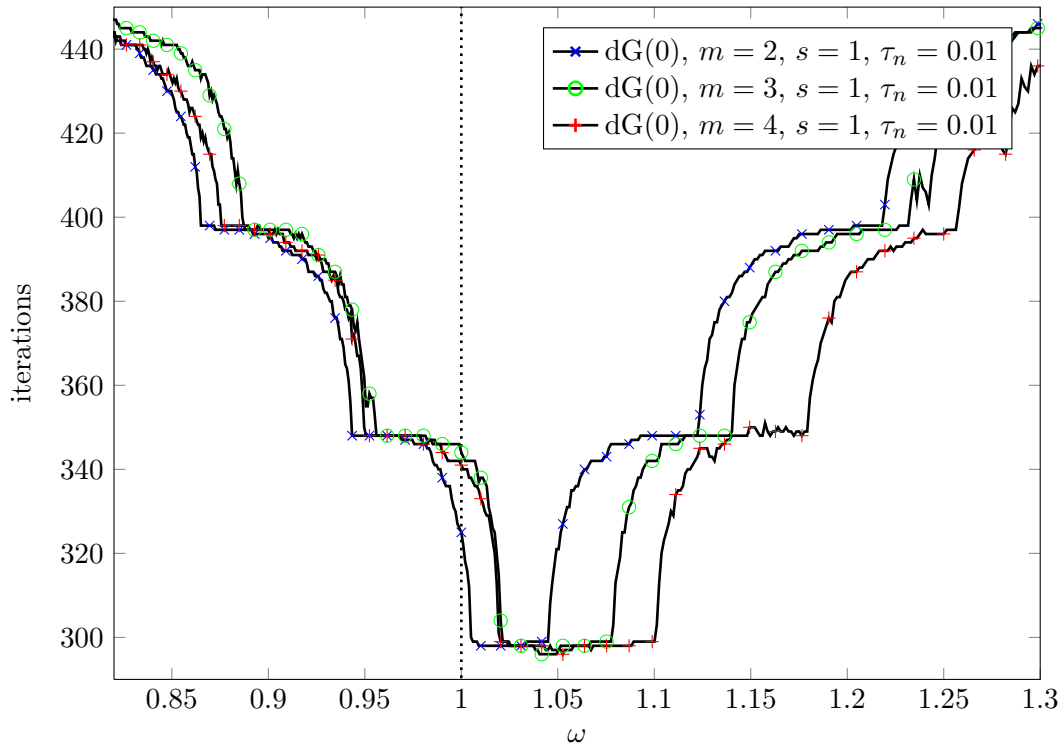


Figure 5.2: Total fixed-stress iterations for varying mesh size  $h = 2^{-(m+1)}$  for dG(0) in time.

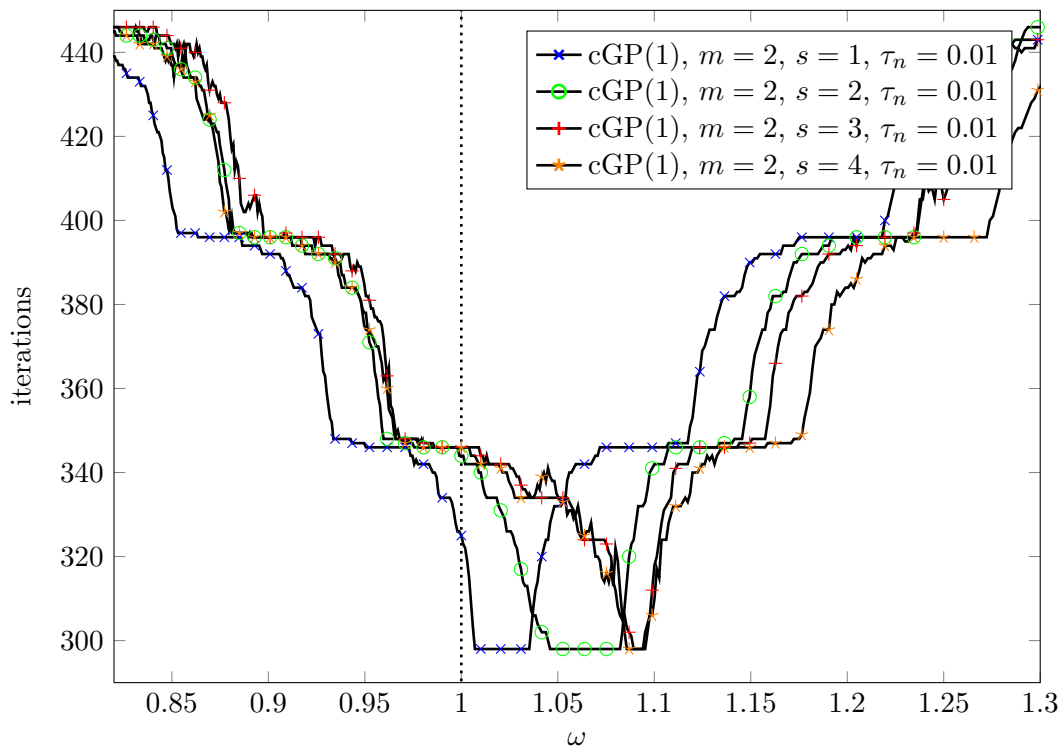


Figure 5.3: Total fixed-stress iterations for varying polynomial degree  $s$  for cGP(1) in time.

a value of  $\omega$  slightly greater than  $\omega = 1$  seems to be advantageous. Nevertheless, the great impact of our analysis for the choice of the optimal numerical parameter  $L$  is obvious.

Next, in our third numerical study the sensitivity (cf. Fig. 5.4) of the iteration process with respect to the choice of the time step size is analyzed. This is done for the dG(1) time discretization scheme; cf. Sec. 3.2. Halvening the time step size and thereby doubling the number of time steps doubles the total number of iterations for the fixed-stress splitting solution in the interval  $I$ . Again, the results of our analyses in Sec. 2 for the continuous case and in Sec. 4 for the discrete case are confirmed by the illustrated dependence of the number of iterations on the perturbation  $\omega$ . No significant difference is observed in the convergence behavior whether a continuous cGP(1) or discontinuous dG(1) time discretization is applied.

Finally in Fig. 5.5 the same study is presented for the higher order cGP(2) approach with a continuous approximation in time with piecewise quadratic polynomials. For comparison the total number of iterations depending on the perturbation  $\omega$  are illustrated for the cGP(1) and cGP(2) approach. No significant deviations are observed.

Summarizing, we can state that the numerical results nicely confirm our analyses and conjectures given in Sec. 2 and in Sec. 4, respectively. An almost optimal choice of the numerical tuning parameter  $L$  in the fixed-stress iteration schemes (2.7)–(2.9) as well as (3.7)–(3.8) and (3.14)–(3.16) is given by  $L = b^2/(2\lambda)$ . This choice only depends on modelling and not on discretization parameters.

## 6 Summary

In this work we presented and analyzed an iterative splitting scheme for the numerical approximation of the quasi-static Biot system of poroelasticity. For the discretization of the separated subproblems of fluid flow and mechanical deformation space-time finite element methods of arbitrary polynomial order are used. For the approximation of the time variable continuous and discontinuous Galerkin approaches are considered. The convergence of the iterative coupling scheme is shown for the continuous model of partial differential equations and the fully discrete set of algebraic equations. For both cases our analyses propose the same optimal choice of an inherent stabilization or tuning parameter of the iterative approach. In particular, the parameter is independent of the numerical discretization parameters. Our presented numerical results nicely confirm the theoretical results and the expected convergence behaviour. Moreover, they underline the efficiency and stability of the proposed approaches for simulating flow in deformable porous media modelled by the Biot system. Next, we plan to apply the optimized fixed-stress iterative coupling strategy to more complex physical models of flow in deformable porous media. In particular, variably saturated and multiphase flow [25, 33, 35] as well as non-linear poroelasticity are in the scope of our interest.

## Acknowledgements

This work was supported by the German Academic Exchange Service (DAAD) under the grant ID 57238185, by the Research Council of Norway under the grant ID DAADppp255715 and the Toppforsk projekt under the grant ID 250223.



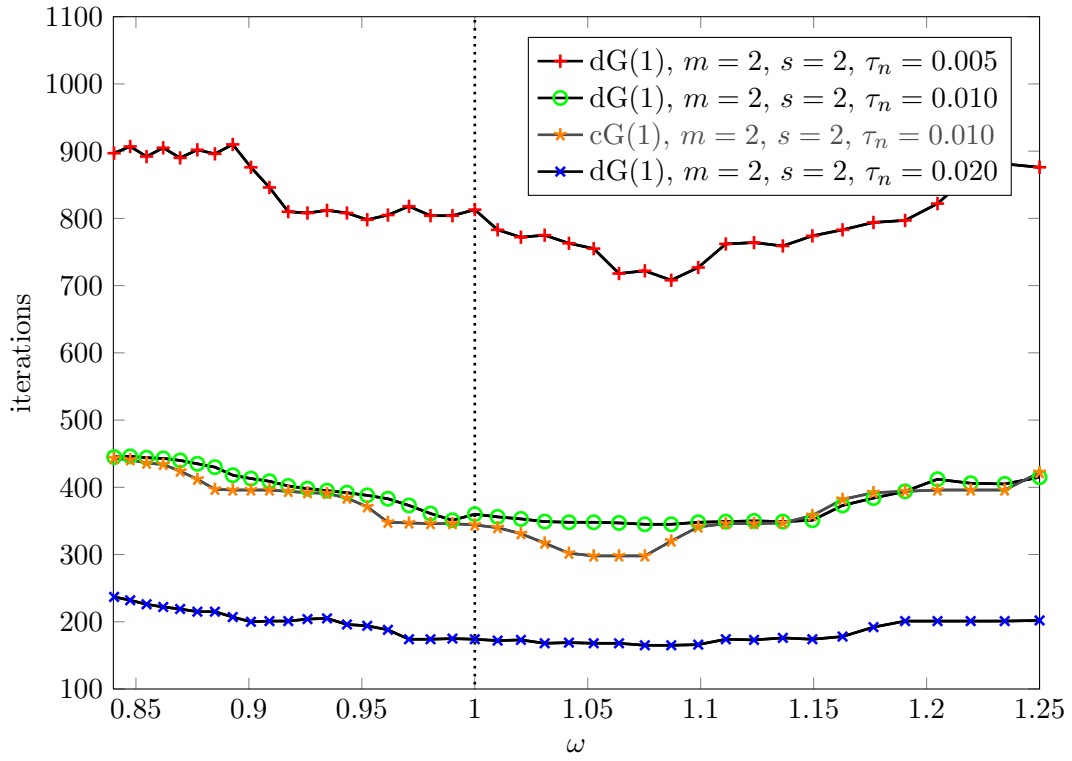


Figure 5.4: Total fixed-stress iterations for varying step length size  $\tau_n$  for dG(1) in time.

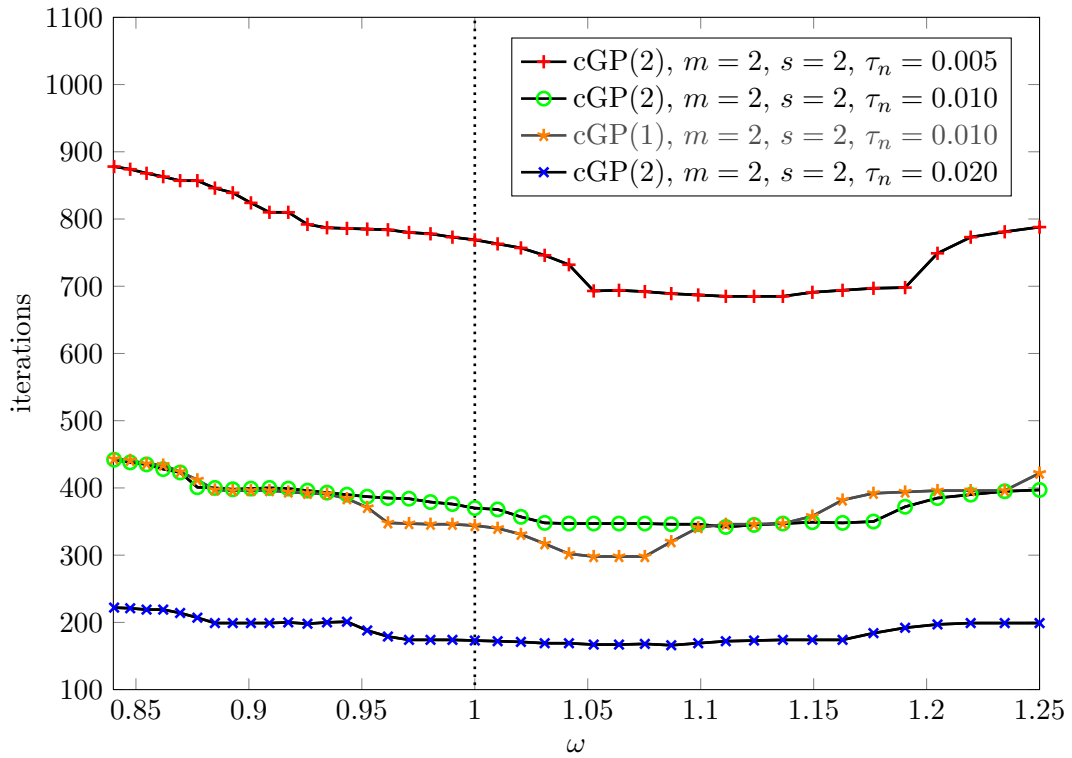


Figure 5.5: Total fixed-stress iterations for varying step length size  $\tau_n$  for cGP(2) in time.

## References

- [1] N. Ahmed, S. Becher, G. Matthies, *Higher-order discontinuous Galerkin time stepping and local projection stabilization techniques for the transient Stokes problem*, *Comp. Meth. Appl. Mech. Eng.*, **313** (2017), DOI: 10.1016/j.cma.2016.09.026.
- [2] N. Ahmed, G. Matthies, L. Tobiska, H. Xie, *Discontinuous Galerkin time stepping with local projection stabilization for transient convection–diffusion–reaction problems*, *Comp. Meth. Appl. Mech. Eng.*, **200** (2011), 1747–1756 .
- [3] T. Almani, K. Kumar, A. Dogru, G. Singh, M. F. Wheeler, *Convergence analysis of multirate fixed-stress split iterative schemes for coupling flow with geomechanics*, *Comp. Meth. Appl. Mech. Eng.*, **311** (2016), 180–207.
- [4] W. Bangerth, R. Rannacher, *Adaptive Methods for Differential Equations*, Birkhäuser, Basel, 2003.
- [5] M. Bause, U. Köcher, *Iterative coupling of variational space-time methods for Biot’s system of poroelasticity*, in B. Karasözen et al. (eds.), *Numerical Methods and Advanced Applications – ENUMATH 2015*, Springer, Berlin, 2016.
- [6] M. Bause, U. Köcher, *Variational time discretization for mixed finite element approximations of nonstationary diffusion problems*, *J. Comput. Appl. Math.*, **289** (2015), 208–224.
- [7] M. Bause, F. A. Radu, U. Köcher, *Error analysis for discretizations of parabolic problems using continuous finite elements in time and mixed finite elements in space*, *Numer. Math.*, **subm.** (2015), <http://arxiv.org/abs/1504.04491>, 1–42.
- [8] N. Castelletto, J. A. White, H. A. Tchelepi, *Accuracy and convergence properties of the fixed-stress iterative solution of two-way coupled poromechanics*, *Int. J. Num. Anal. Meth. Geomechanics*, **39** (2015), 1593–1618.
- [9] N. Castelletto, J. A. White, M. Ferronato, *Scalable algorithms for three-field mixed finite element coupled poromechanics*, *J. Comp. Phys.*, **327** (2016), 894–918.
- [10] Z. Chen, *Finite Element Methods and their Applications*, Springer, Berlin, 2010.
- [11] Y.-Z. Chen, L.-C. Wu, *Second Order Elliptic Equations and Elliptic Systems*, American Mathematical Society, Rhode Island, 1998.
- [12] deal.II, *deal.II – an open source finite element library*, Version 8.4.1, <http://www.dealii.org>, 2016
- [13] V. Dolejší, M. Feistauer, *Discontinuous Galerkin Method*, Springer, Berlin, 2015.
- [14] A. Ern, J. L. Guermond, *Theory and Practice of Finite Elements*, Springer, Berlin, 2010.
- [15] A. Ern, F. Schieweck, *Discontinuous Galerkin method in time combined with an stabilized finite element method in space for linear first-order PDEs*, *Math. Comp.*, **85** (2016), 2099–2129.

- [16] L. C. Evans, *Partial Differential Equations*, American Mathematical Society, Providence, Rhode Island, 2010.
- [17] S. Hussain, F. Schieweck, S. Turek, *Higher order Galerkin time discretization for nonstationary incompressible flow*, in A. Cangiani et al. (eds.), *Numer. Math. and Adv. Appl.* 2011, Springer, Berlin, 509–517, 2013.
- [18] S. Hussain, F. Schieweck, S. Turek, *A note on accurate and efficient higher order Galerkin time stepping schemes for nonstationary Stokes equations*, *The Open Numer. Meth. J.*, **4** (2012), 35–45.
- [19] B. Jha, R. Juanes, *A locally conservative finite element framework for the simulation of coupled flow and reservoir geomechanics*, *Acta Geotechnica*, **2** (2007), 139–153.
- [20] O. Karakashin, C. Makridakis, *A space-time finite element method for the nonlinear Schrödinger equation: the continuous Galerkin method*, *SIAM J. Numer. Anal.*, **36** (1999), 1779–1807.
- [21] J. Kim, H. A. Tchelepi, R. Juanes, *Stability and convergence of sequential methods for coupled flow and geomechanics: Drained and undrained splits*, *Comput. Methods Appl. Mech. Engrg.*, **200** (2011), 2094–2116.
- [22] U. Köcher, M. Bause, *Variational space-time methods for the wave equation*, *J. Sci. Comput.*, **61** (2014), 424–453.
- [23] U. Köcher, *Variational space-time methods for the elastic wave equation and the diffusion equation*, PhD Thesis, Helmut-Schmidt-Universität, <http://edoc.sub.uni-hamburg.de/hsu/volltexte/2015/3112/>, 2015.
- [24] J. Lee, *Robust finite element methods for Biot’s consolidation model*, in A. Logg, K. A. Mardal (eds.), *Proceedings of the 26th Nordic Seminar on Computational Mechanics*, Center for Biomedical Computing, Simula Research Laboratory, Oslo, 123–126, 2013.
- [25] F. List and F. A. Radu, *A study on iterative methods for solving Richards’ equation*, *Comput. Geosci.*, **20** (2016), 341–353.
- [26] A. Mikelić, M. F. Wheeler, *Theory of the dynamic Biot–Allard equations and their link to the quasi-static Biot system*, *J. Math. Phys.*, **53** (2012), 123702:1–15.
- [27] A. Mikelić, M. F. Wheeler, *Convergence of iterative coupling for coupled flow and geomechanics*, *Comput. Geosci.*, **17** (2013), 479–496.
- [28] A. Mikelić, B. Wang, M. F. Wheeler, *Numerical convergence study of iterative coupling for coupled flow and geomechanics*, *Comput. Geosci.*, **18** (2014), 325–341.
- [29] J. M. Nordbotten, *Stable Cell-Centered Finite Volume Discretization for Biot Equations*, *SIAM J. Numer. Anal.*, **54** (2016), 942–968.
- [30] P. J. Philips, M. F. Wheeler, *A coupling of mixed and continuous Galerkin finite element methods for poroelasticity I, II*, *Comput. Geosci.*, **11** (2007), 131–158.

- [31] P. J. Philips, M. F. Wheeler, *A coupling of mixed and discontinuous Galerkin finite element methods for poroelasticity*, *Comput. Geosci.*, **12** (2008), 417–435.
- [32] P. J. Philips, M. F. Wheeler, *Overcoming the problem of locking in linear elasticity and poroelasticity: an heuristic approach*, *Comput. Geosci.*, **13** (2009), 5–12.
- [33] I. S. Pop, F. A. Radu, P. Knabner, *Mixed finite elements for the Richards’ equation: linearization procedure*, *J. Comput. Appl. Math.*, **168** (2004), 365–373.
- [34] A. Quarteroni, A. Valli, *Numerical Approximation of Partial Differential Equations*, Springer, Berlin, 2008.
- [35] F. A. Radu, J. M. Nordbotten, I. S. Pop, K. Kumar, *A robust linearization scheme for finite volume based discretizations for simulation of two-phase flow in porous media*, *J. Comput. Appl. Math.*, **289** (2015), 134–141.
- [36] C. Rodrigo, F. J. Gaspar, X. Hu, L. T. Zikatanov, *Stability and monotonicity for some discretizations of the Biot’s consolidation model*, *Comp. Meth. Appl. Mech. Eng.*, **298** (2016), 183–204.
- [37] F. Schieweck, *A-stable discontinuous Galerkin–Petrov time discretization of higher order*, *J. Numer. Math.*, **18** (2010), 25–57.
- [38] A. Settari, F. M. Mourits, *A coupled reservoir and geomechanical simulation system*, *SPE Journal*, **3**(3) (1998), 219–226.
- [39] R. Showalter, *Diffusion in poro-elastic media*, *J. Math. Anal. Appl.*, **251** (2000), 310–340.
- [40] R. Showalter, U. Stefanelli, *Diffusion in poro-elastic media*, *Math. Meth. Appl. Sci.*, **27** (2004), 2131–2151.
- [41] V. Thomeé, *Galerkin Finite Element Methods for Parabolic Problems*, Springer, Berlin, 2006.
- [42] J. A. White, N. Castelletto, H. A. Tchelepi, *Block-partitioned solvers for coupled poromechanics: A unified framework*, *Comp. Meth. Appl. Mech. Eng.*, **303** (2016), 55–74.